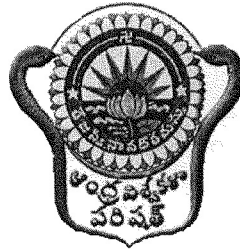Workshop on the future of ionospheric research for Satellite Navigation and Positioning: its relevance for developing countries

4 – 15 December 2006

Characteristics of the Indian equatorial ionosphere

Lecture Notes

Prof. P.V.S. Rama Rao

Department of Physics
Andhra University
Visakhapatnam - 530 003
INDIA

Contents

Climatology of Equatorial Ionosphere over Indian Sector

1 Equatorial Ionosphere

1.1 Introduction

The absorption of solar EUV radiation by the Earth's upper atmosphere (about 80 km to about 1000 km) leads to atmospheric heating, photo dissociation of molecular species and creation of free electrons and ions through photo ionization. The electrons and ions (10^4 to 10^6 ele/cm^3) constitute the electrically conducting ionosphere with the neutral atmosphere (10^{13} ele/cm^3) (thremosphere) dominating the background. The differential heating of the thermosphere on the day and night side hemispheres creates horizontal pressure gradients and the resultant global neutral wind system effectively distributes momentum and energy. The movement of the electrically conducting upper atmosphere across the geomagnetic field by thermospheric zonal winds generates electric fields as in a dynamo, and this is central to the electrodynamics of Equatorial Ionosphere.

The equatorial and low latitude ionosphere is the region where the Earth's magnetic field lines are nearly horizontal. Due to the unique configuration of mutually perpendicular electric field (east-west), magnetic field (north-south) and electron density gradient (upward), the equatorial ionosphere is more susceptible for most important electrodynamical phenomena such as (i) Equatorial ElectroJet (EEJ), (ii) Counter Equatorial ElectroJet (CEEJ), (iii) Equatorial Ionization Anomaly (EIA), (iv) Equatorial Spread-F (ESF) and (v) Midnight Temperature Maximum (MTM).

1.2 Equatorial ElectroJet (EEJ)

Equatorial ElectroJet is an intense band of current flowing in the east-west direction at the dip equator with latitudinal extent of $\pm 3^\circ$ on either side of the dip equator (i.e., ± 300 km) and in the height region of $100 - 110$ km with maximum current flowing at 105 km present during both day and night. This current is driven primarily by the dynamo action of the neutral wind and is responsible for the strong enhancement in the horizontal component (H) of Earth's magnetic field observed by the magneto meters over the equator as shown in Figure.1.

The difference between the ΔH values (H-component of the magnetic field after subtracting the night time base level) over the equator and a location of about 6-10° dip latitude is taken as a measure of Equatorial ElectroJet (EEJ) strength (Rastogi and Klobuchar, 1990) as shown in Figure. 2.
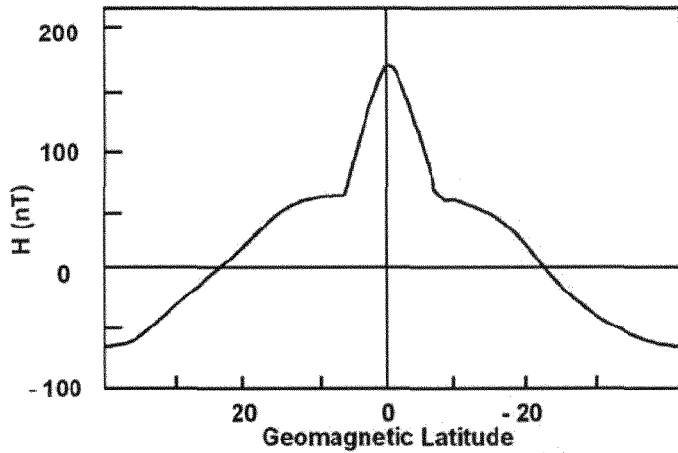
Figure 1. Schematic plot of typical noontime magnetometer H component observations as a function of latitude. (after Anderson et al., 2002.)
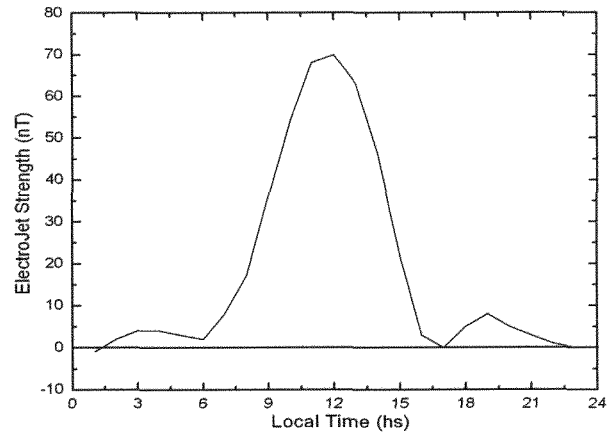
Figure 2. ElectroJet strength variation as measured by the difference in ΔH values between Trivandrum (8.5°N, 77°E. 0.5°S dip) and Alibag (18.5°N, 72.9°E, 13°N dip)

1.3 Counter Equatorial ElectroJet (CEEJ)

At times on magnetically quiet days, the post-noon decrease of ΔH at an equatorial station becomes abnormally rapid and large to such an extent that the ΔH value becomes negative for sometime and then it recovers back to its normal positive value before its decrease towards zero again around sunset time (Gouin, 1962, Gouin and Mayaud, 1967). The event lasts for about 3 hours and the maximum negative value of ΔH usually occurs between 1500 and 1600 hrs local times (Krishnamurthy and Sengupta, 1972, Rastogi, 1973). This phenomenon is termed as the 'Counter Equatorial ElectroJet', as the electrojet current then reverses and flows westward as shown in Figure. 3. There are two possible explanations on how the electrojet current reverses. First, the possible reversal of the vertical polarization electric field E_p in the entire height range of the EEJ due to the local interaction of height-varying winds has been sought (Richmond, 1973, Fambitakoye et al., 1976, Ananda Rao and Raghava Rao, 1987 and references therein).
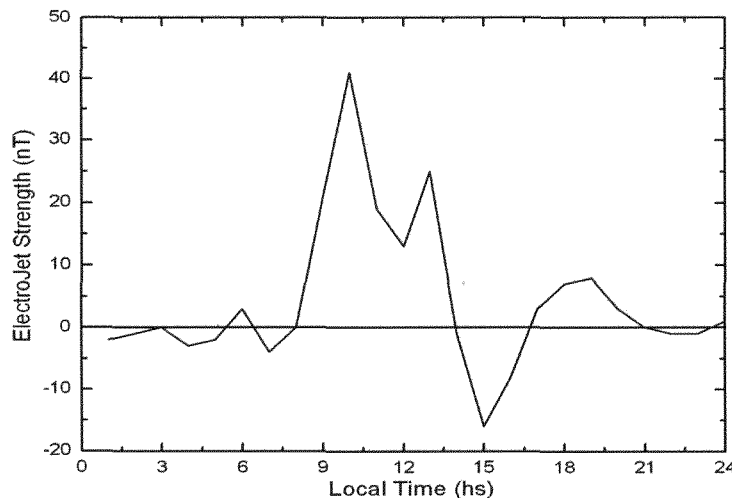
Figure 3

Typical example of Counter ElectroJet event

4

Secondly, the possible reversal of the east-west electric field E_y in the EEJ due to an abnormal combination of global scale tidal wind modes generating reversed E_y has been sought with considerable success (Forbes and Lindzen, 1976, Schieldge et al., 1973). However, the real physical mechanisms of CEEJ are yet to be understood completely, and so are the implications of this process in controlling the dynamics of the low and equatorial upper atmosphere. The occurrence of afternoon CEEJ is more frequent during solar minimum periods and inversely varies with sunspot cycle.

1.4 Equatorial Ionization Anomaly (EIA) and Fountain Effect

During the equinox the sun is overhead at the equator, and in terms of solar control the ionization density is expected to be maximum in that region. Instead, the daytime ionization density at the F_2 peak shows a pronounced trough at the magnetic equator and crests at about 30°N and 30°S magnetic dip. This anomalous latitudinal variation of F_2 ionization near the magnetic equator obtained from bottomside ionograms illustrated in Figure. 4, was first recognized by Appleton (1946) and is known as the Equatorial Ionization Anomaly (EIA) or Appleton anomaly.
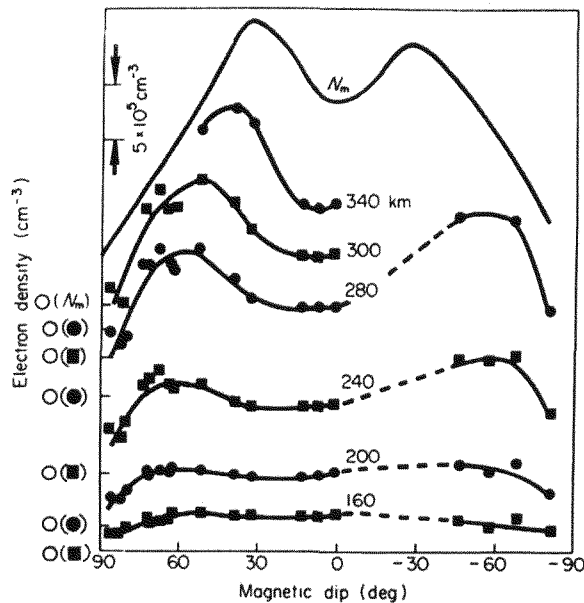
Figure. 4. Variation of NmF$_2$ and of electron density at fixed heights with magnetic dip for noon time on magnetically quiet days in Sep,1957

The equatorial anomaly is explained in terms of a *fountain effect* caused by the vertical electrodynamic drift at the equator and plasma diffusion away from the equator along the geomagnetic field lines. Figure. 5 illustrates how the eastward E-region

dynamo electric field at locations slightly off the magnetic equator maps to F-region altitude over the equator.
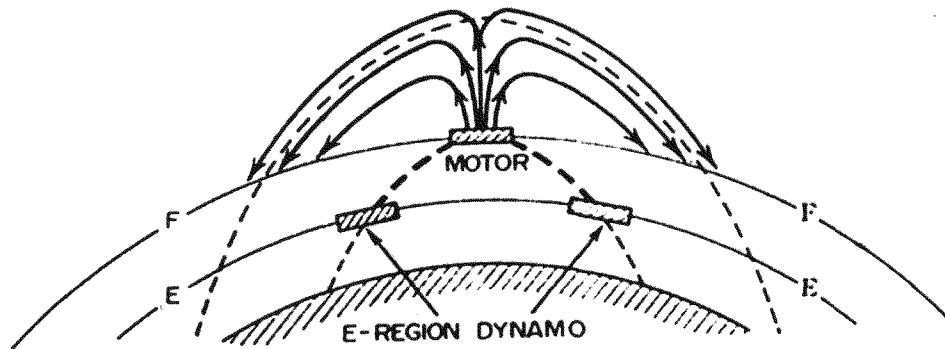
Figure. 5. Near the equator the electric fields of the atmospheric dynamo in the E layer are conveyed upwards along geomagnetic lines of force to the motor in the F layer where they produce an upwards movement of the plasma during the day

The eastward electric field in conjunction with the north-south geomagnetic field lines gives rise to a vertically upward plasma motion. As the plasma rise, it encounters the horizontal lines of force of the Earth's magnetic field. The electrons diffuse along these field lines and reenter the main body of the ionosphere where the field lines cut through the F region, giving rise to large clumps of ionization at magnetic latitudes of ± 15-20° on either side of the magnetic equator as illustrated in Figure. 6. These clumps are called the peaks or **crests,** and the depleted ionization region over the equator is called **trough** of the equatorial or Appleton anomaly.
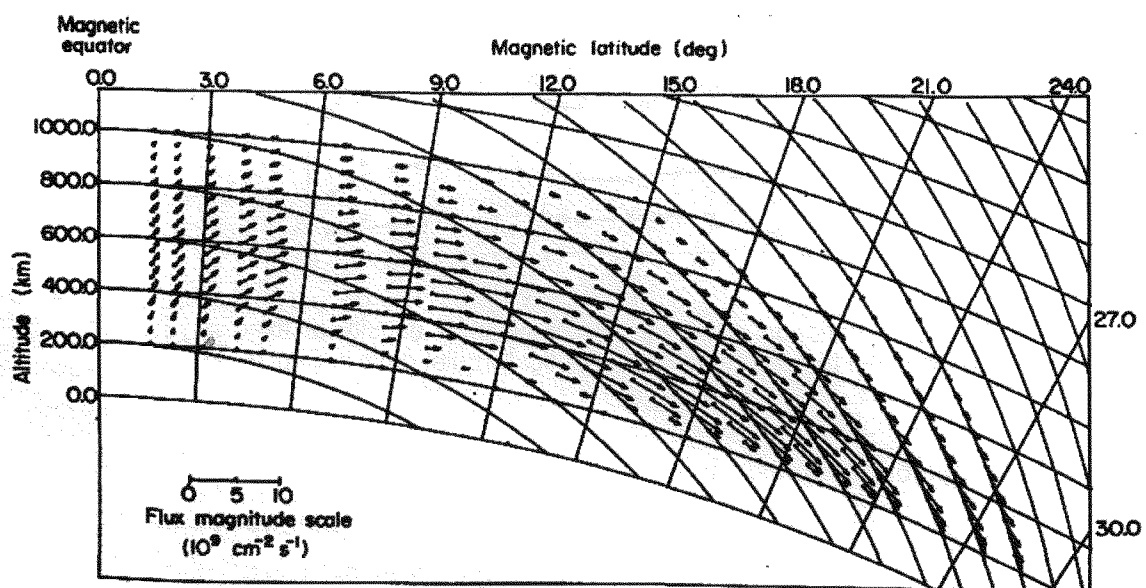
Figure. 6. The fountain effect causing the upward drift of electrons under the combined influence of horizontal electric and magnetic fields, then diffuse down along lines of force of the Earth's magnetic field towards lower altitudes and higher latitudes.

The diurnal development of the crests revealed that they become more pronounced by 1200-1400 LT during solar minimum and at 1900-2100 LT during solar maximum. During the latter, the abnormal enhancement of EIA in the post sunset hours is due to the resurgence of fountain effect because of post sunset enhancement in the eastward electric field before the reversal, and the crests were found to survive into the night by returning to the equator around 0300 LT (Rastogi, 1966).

1.5 Equatorial Spread-F (ESF)

The night time equatorial F-region often consists of plasma density irregularities, which manifest themselves as diffused echoes on ionograms, known as Spread-F, rapid fluctuations in the amplitude and phase of the trans-ionospheric radio wave signal, known as scintillations, density depletions in the rocket experiments, plume like structures in the HF/VHF radar maps and airglow intensity bite outs in the optical experiments, are called under the generic name of **Equatorial Spread-F (ESF)**.

The primary process responsible for the development of large scale ESF irregularities is gravitationally driven by Rayleigh-Taylor (GRT) instability mechanism operating in the post sunset bottomside F-region. A hierarchy of plasma instabilities is believed to be responsible for the generation of wide range of scale sizes few centimeters to several hundred kilometers through secondary plasma processes. The growth rate γ_{RT} of GRT instability (neglecting the chemical recombination) is given as (Martinis et al. 2005)

$$\gamma_{RT} = \frac{\Sigma_P^F}{\Sigma_P^E + \Sigma_P^F} \, \frac{\vec{\nabla} N}{N} \cdot \left[\frac{\vec{E} \times \vec{B}}{B^2} + \frac{\vec{g}}{\nu_{in}} - \vec{U}_n \right] \qquad \text{-------- (1)}$$

$$(a) \qquad (b) \qquad (c) \qquad (d) \quad (e)$$

If the growth rate is positive, the instability will develop and a spectrum of irregularities are generated within a few $(\gamma_{RT})^{-1}$ time scales (tens of minutes to $\approx$ 1 hour). For ESF to develop, there are five processes that might be subdivided into two enabling conditions and three driving/suppressing effects represented as (a) through (e) in Equation (1). The enabling effects occur after sunset, when the F region to total (E + F) region Pedersen conductivity ratio (a) approaches unity and the electron density gradient, $\Delta N/N$ (b) is large. Upward E X B drifts (c) have been observed to be the main drivers for the generation of ESF. It is generally accepted that a strong upward drift in the post sunset period is the single most important condition for ESF to occur [Fejer et al., 1999; Mendillo et al., 2001]. Enhancing effects occur when the ionosphere moves to high

altitudes, reducing the collision frequency between ions and neutrals v_{in} and thus causing (d) to be large. The neutral wind term (e) refers to the component perpendicular to the magnetic field. In the context of flux tube integrated analysis Un = Um sin I + Uv cos I, where Um and Uv are the meridional and vertical components of the total wind in the geomagnetic meridian and I is the magnetic inclination angle. There is no conclusive observational evidence to support a role of day-to-day changes in meridional neutral winds upon ESF [Mendillo et al., 2001], while simulations tend to include it as a suppressant for ESF.

1.6 Scintillations

Radio waves from satellites or radio stars during their passage through the ionospheric irregularities of electron density develop random phase fluctuations across the wavefront. As the wavefront travels towards the ground, phase mixing occurs and, as a result, not only phase but amplitude fluctuations as well, develop on the ground (Fig.7). Due to the relative motion between the satellite, ionospheric irregularities and the receiver on ground, the spatial pattern of amplitude and phase variations sweeps past the receiver and the temporal variations of phase and amplitude known as scintillations are recorded at the ground (Fig. 8).
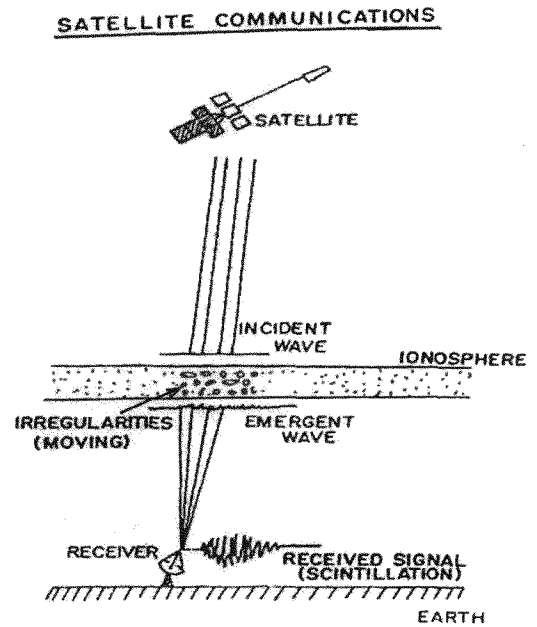

Figure. 7 Geometry of the scintillation problem
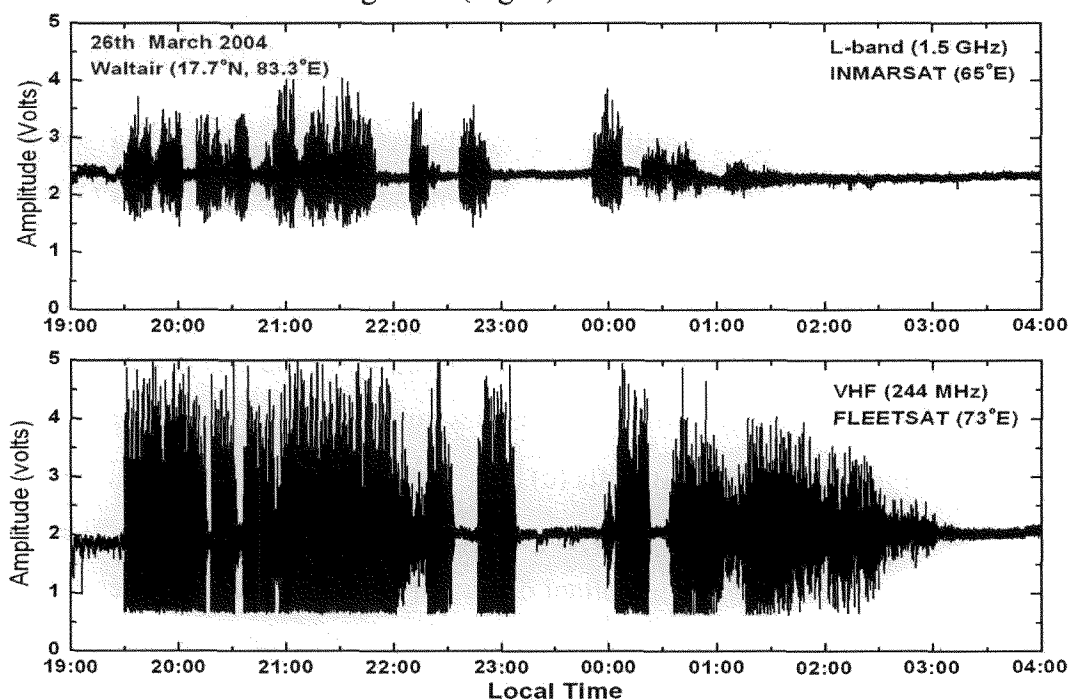
Figure. 8 Typical amplitude scintillations recorded at 1.5 GHz (top panel) and 244 MHz (bottom panel) from two geo-stationary satellites INMARSAT (65°E) and FLEETSAT (73°E) on 26th March 2004.

8

The amplitude and phase fluctuations of the recorded signal are statistically characterized by two major parameters, amplitude and phase scintillation indices, denoted respectively by S4 and $\sigma\phi$. The amplitude scintillations index (S4) is defined as the square root of the variance of received power divided by the mean value of the received power (Briggs and Parkin, 1963)

$$\text{i.e., } S4 = \frac{\sqrt{(<I^2> - <I>^2)}}{<I>} \quad \text{------------} \quad (2)$$

The phase scintillation index ($\sigma\phi$) is defined as the standard deviation of a linearly detrended phase data segment.

$$\text{i.e., } \sigma\phi = \sqrt{(<\phi^2> - <\phi>^2)} \quad \text{-----------} \quad (3)$$

Scintillations is the most simple and inexpensive diagnostic tool for characterizing the general morphological features of Equatorial Spread-F (ESF), hence is widely used world over.

1.7 Morphological features of ESF

The Equatorial Spread-F (ESF) is essentially a night time phenomenon and occurrence of ESF is highly variable from day-to-day and is largely controlled by local time, season, solar cycle, latitude, longitude and geomagnetic activity. A new irregularity patch or plasma bubble develops after sunset by expanding westward in the direction of the solar terminator with velocities similar to that of the terminator. It comes to an abrupt halt after typically expanding to an east-west dimension of 100 to several hundred kilometers. The vertical thickness of the patch is 50 to several hundred kilometers, and in general the patch encompasses a height region from 200 to 450 km, although irregularities have been observed to exist up to 1000 km altitude. When they become field aligned the north-south dimension of the irregularity patch is of the order of 2000 km or greater. Once the patch is fully formed, they drift eastward with velocities ranging from 100 to 200 m/s (Aarons et al. 1980).

When the irregularity patch is extended to the latitude of the anomaly crest, the irregularities will encounter highest levels of background electron density, so that the trans-ionospheric radio wave propagation through this intersection undergoes the highest disruptive levels of scintillation, both in amplitude and in phase.

2. Spatial and temporal characteristics of L-band scintillations over the Indian low latitude region and their possible effects on GPS navigation

2.1 Introduction

The Global Positioning System (GPS) is a satellite based navigation system, which provides a good positional accuracy of the user at any point of the globe, and at any given time using the L-band frequencies of L1 (1575.42 MHz) and L2 (1227.60 MHz). The GPS positioning accuracies are subjected to various effects like clock biases of the satellites and receivers, ionospheric and tropospheric delays, and receiver noise. Among these, the effects of accuracy degradation due to group delay introduced by ionospheric total electron content (TEC) and ionospheric scintillations caused by small scale density irregularities are the most significant. Therefore the standalone GPS is not suitable for certain navigation applications like aircraft's landing using Category-I (CAT-I) precision approach. In Indian region the augmenting of GPS is planned through regional Satellite Based Augmentation System (SBAS), called GPS Aided Geo Augmented Navigation (GAGAN) by Indian Space Research Organisation (ISRO) and Airport Authority of India (AAI).

Most of the Indian region encompasses the equatorial and low latitude ionospheres. The morphology of the equatorial ionosphere is quite different from that of other latitudes because the magnetic field (B) at the equatorial region is nearly parallel to the Earth's surface. During daytime, the E-region dynamo electric field (E) is eastward. This field in the E region and at off-equatorial latitudes maps along the magnetic field to F-region altitudes above the magnetic equator resulting in E x B drift, which transports F-region plasma upward over the magnetic equator. The uplifted plasma over the equator then moves along magnetic field lines in response to gravity, diffusion, and pressure-gradient forces. As a result, the equatorial ionization anomaly is formed with reduced F-region ionization density at the magnetic equator and increased ionization at the two anomaly crests around $\pm15°$ in magnetic latitude to the north and south of the magnetic equator.

It is known that near sunset, the dynamics of the equatorial ionosphere are dominated by the pre-reversal enhancement (PRE) (Woodman, 1976) of the vertical drift at the equator. During sunset, plasma densities and dynamo electric fields in the E region decrease, and the anomaly begins to fade, and at this local time a dynamo electric field develops in the F-region. Polarization charges set up by the conductivity gradients at the

terminator enhance the eastward electric field for about an hour after sunset. With the decreased ionization density in the E-region after sunset, vertical plasma density gradients form in the bottom side of the F layer, resulting in the upward density gradients opposite in direction to the gravitational force. This configuration is Rayleigh-Taylor (RT) unstable and allows plasma density irregularities to generate (Kelley et al, 1981, 1986; Huang and Kelley 1996; Hysell 2000). The eastward post-sunset electric fields enhance the R-T instability, while westward fields quench it. These irregularities can grow to become large ionospheric depletions often called equatorial plasma bubbles, which are elongated along the magnetic flux tubes. The variability in the PRE may dictate the onset or inhibition of these instabilities (Basu et al., 1996; Hysell and Burcham, 1998; Fejer et al., 1999). The Indian region covers latitudes ranging from the magnetic equator to the northern anomaly crest and beyond up to 27° N geomagnetic latitudes, and it is also known that scintillations are most severe at the locations around the anomaly crest where the electron density gradients are high (Aarons et al., 1981; Basu et al., 1988).

Small-scale irregularities in the electron content of the ionosphere, with spatial extents from a few metres to a few kilometres, can produce both refraction and diffraction effects on received GPS signals. The refraction changes the direction and speed of propagation of an electromagnetic wave, and the diffraction gives rise to spatial fluctuations in the amplitude and phase of the received signal. The movement of the ionospheric irregularities relative to the signal path converts these spatial fluctuations due to diffraction effects into temporal fluctuations. And these fluctuations due to the diffraction effects are observed as scintillations in the GPS received signal (Wanninger, 1993). It was observed that during strong scintillation, deep amplitude fades or large phase fluctuations may cause signal disruptions in the receiver- satellite link (Skone et al., 2000; Kintner et al., 2001). Amplitude scintillations can be monitored by the time series of C/N_0 (signal to noise ratio) provided by the GPS output, and phase scintillations result from sudden changes in ionospheric refraction or from diffraction effects. The strong amplitude scintillation may cause the received signal power to drop below the receiver's threshold limit, and then a loss of lock is observed. The strong phase scintillation may cause Doppler shift in frequency in the received signal carrier exceeding the receiver's phase-lock-loop (PLL) bandwidth, resulting in a loss of phase lock of the receiver. It was observed that phase scintillations are always accompanied by atleast

moderate levels of amplitude scintillations (Doherty et al., 2004). Both the amplitude and phase scintillations increase the root-mean-square (RMS) phase-tracking error in the output of the PLL, when the RMS jitter exceeds a threshold, loss of lock may occur even if the signal is above the threshold of the receiver (Knight and Finn, 1988; Conker et al., 2003). A decrease in the number of GPS signals locked by a user receiver can result in poor navigation accuracy. And moreover, loss of signal lock at SBAS monitoring stations can degrade the broadcast correction information.

First time, we report scintillation characteristics observed at the L-band frequency of 1.575 GHz over the entire Indian region using an eighteen-month data for the period from January 2004 to July 2005 from a network of eighteen GPS receiver stations in India. We present here the results on the spatio-temporal and intensity characteristics of the L-band scintillations (S4 index), simultaneously measured by these receivers in the Indian region and the possible effects on GPS navigation.

2.2 Data and method of analysis

In the present study the amplitude scintillation (S4 index) data at 1.575 GHz recorded by the dual frequency GPS receivers installed at the 18 different locations in the Indian region under the Indian GAGAN programme during the eighteen-month period from January 2004 to July 2005 are used. The chain of receivers are installed such that they cover the Indian region from the magnetic equator to the equatorial anomaly crest and beyond, at a grid spacing of about 5° x 5° in latitude and longitude as depicted in Fig. 9. Here the longitudinal coverage of these stations vary from 72° E to 92° E, and the geographic latitudes vary from 8° to 32° N covering a range of 1° S to 23° N magnetic latitudes.

The GSV 4004 Ionospheric Scintillation Monitor receivers (ISMs) are used to collect the TEC and scintillation data (Van Dierendonck et al., 1996). Each ISM can track up to 11 GPS C/A-code signals at the L1-frequency of 1.575 GHz. The data is collected at one minute intervals, which do not include the 50 Hz sampled raw data, but did include statistical data for all satellites being tracked. The statistical data includes parameters like signal to noise ratio (C/N_0), standard deviation parameters of amplitude and phase, receiver lock time, and such other information for each satellite. The ISM calculates the standard deviation of phase fluctuation (phase-sigma) and that of signal intensity fluctuation normalized by its mean (S_4) from raw data sampled at 50 Hz rate. S_4 index is calculated from the normalized standard deviation of raw signal intensity (S_{4T}) and that of ambient noise ($S_{4,NO}$) by the formula $S4 = Sqrt((S_{4T})^2 - (S_{4,NO})^2)$. It was

specified that the phase parameters should be discarded for any lock time less than 240 seconds to allow the detrending filter to resettle, as it should be reinitialized whenever lock is lost.
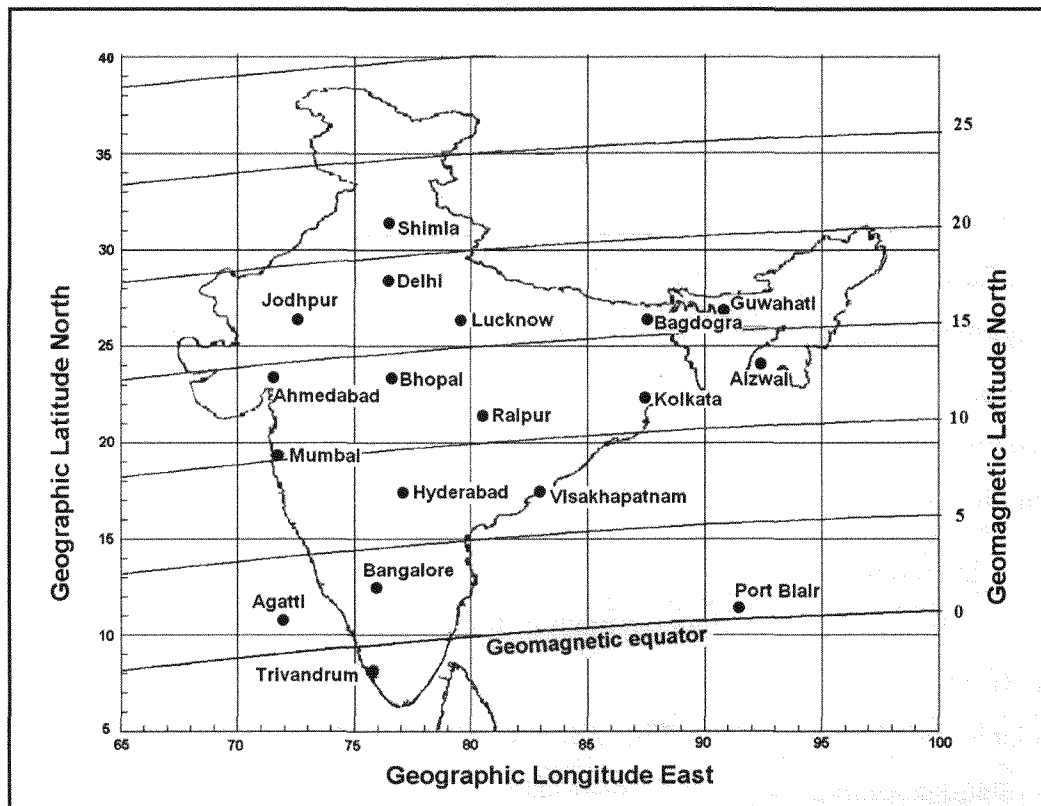
Figure 9. *Location of the GPS receiver installations in the Indian region.*

The scintillation index (S4) and TEC data thus recorded using the GPS receivers are processed for each of the satellite passes with an elevation mask angle greater than 40° so that the effects of low elevation angles such as tropospheric, water vapour scattering and multipath effects are avoided. At low elevation angles high S4 index values are observed (even during daytime hours), because the amplitude scintillation depends on the electron density deviations and on the thickness of the irregularity layer, both of which increase apparently at low elevation angles, causing stronger scintillations, and high S4 index values due to multipath effects. The 40° mask angle may reduce the number of satellites available for actual Satellite Based Augmentation System (SBAS) operation, but allows studying the effects of ionospheric irregularities alone on the GPS navigation limiting the tropospheric and multipath effects at the low elevation angles.

2.3 Results
2.3a L-band scintillations in Indian region

In the recent years, with the increasing demand for the trans-ionospheric communications in the navigation of space borne vehicles such as satellites, aircrafts and surface transportation systems, the study of ionospheric scintillations, particularly at the L-band frequencies (which is commonly used in these systems), has gained importance. It is well known that the scintillations are severe at the low latitude and equatorial regions during the equinox months and during high sunspot activity (HSSA) periods (Aarons, 1982; Basu et al., 1988; Aarons, 1993). The Indian region includes the magnetic equator, the northern anomaly crest region and beyond up to 27° N geomagnetic latitudes. Therefore, the scintillation activity is severe for more than half of the area (equatorial ionization anomaly region) in the Indian Flight Information Region (FIR) as may be seen from Fig. 12.

Therefore, with a view to examine the nature of occurrence of scintillations over the entire Indian region at any give point of time, plots of S4 index as a function of local time (from 18 to 06 hrs LT) are made for all the 18 stations for each day from all the available satellite passes. In Fig. 10, are presented the day to day occurrence of scintillations during the month of March 2004 for four typical stations, namely, Trivandrum (8.4° N geographic latitude, 0.47° S geomagnetic latitude), Waltair (17.7° N G., 8.22° N G.M), Raipur (21.1° N G., 12.78° N G.M) and Jodhpur (26.2° N G., 17.6° N G.M) representing the four different latitude zones in the Indian sector. Trivandrum is an equatorial station, Waltair is a sub-tropical station situated at the inner edge of the equatorial ionization anomaly (EIA), Raipur is a station situated in the crest region of the anomaly, whereas Jodhpur is situated beyond the anomaly crest region. The power levels of the scintillation recorded (S4 index) presented in Fig. 10 are divided into three categories, namely weak (3 to 6 dB, i.e., S4 = 0.17 to 0.3), moderate (6 to 10 dB, i.e., S4 = 0.3 to 0.45) and strong (S4 >10 dB) scintillations respectively.

It may be seen from Fig. 10(a), which shows the scintillation occurrence at the equatorial station, Trivandrum, the occurrence of weak scintillations (3 to 6 dB) are more with practically no occurrence of strong (>10 dB) scintillations. Whereas at Waltair a station situated at the inner edge of the equatorial anomaly crest (Fig. 10b), the occurrence of scintillations at all the three power levels is high. At Raipur (Fig. 10c), a station situated at the crest of the anomaly, the occurrence of strong scintillation is

highest. At Jodhpur (Fig. 10d), a station situated beyond the anomaly crest region, the scintillation activity has considerably decreased to a minimum. The set of these four figures clearly indicates that strong (>10 dB) scintillations occur at and around the EIA region owing to the presence of short scale length (~ few hundred metres) irregularities and high ambient electron densities accompanied by large electron density gradients even during the low sunspot activity (LSSA) period of March 2004. On the other hand, it may be noticed that the occurrence of weak scintillations over the magnetic equator, Trivandrum is maximum compared to the occurrence of weak scintillations at the crest region. Here it may be mentioned that due to the geographic shape of India, the number of GPS receiver stations are less, limiting the spatial coverage (added to that lack of data from 13th to 17th March 2004), around the equatorial region compared to the crest region. Hence the weak scintillation activity is not prominently visible to the extent expected in Fig 10(a). The occurrence of weak scintillations is due to the presence of large scale size irregularities, low ambient electron densities and low electron density gradients at the equator during the LSSA periods. Whereas at the anomaly crest regions, the accumulated F- region ionization, transported from the equator, is high resulting in high electron density gradients and small scale irregularities giving rise to the generation of strong scintillations at the L-band frequency of 1.5 GHz.

In Figs. 11 a, b & c are presented the percentage occurrence of scintillations as contour diagrams at the three different power ranges, over the entire country, with a view to study the latitudinal variation as a function of local time for the equinoxial month of March 2004. It may be seen from Fig. 11(a) that the percentage occurrence of weak (3 to 6 dB) scintillations is maximum (58%) with peak occurrence around 21 hrs LT. at 17° N geographic latitude. The percentage occurrence of moderate (6 to 10 dB) scintillations (Fig. 11b) is relatively low with peak occurrence (44%) confining to 21 hrs LT. at latitudes of 15° to 20° N. Whereas strong (>10 dB) scintillations presented in Fig. 11(c) the percentage occurrence is lowest (37%) compared to weak and moderate scintillations. The peak occurrence of strong scintillations during this month (March 2004) is confined to 17° N geographic latitude and to the local time of 21 hrs. From Figs. 10 and 11 it may be noticed that most of the L-band scintillations in the Indian region occur during the pre-midnight period of 19-24 hours LT. with scanty occurrence during post-midnight hours.
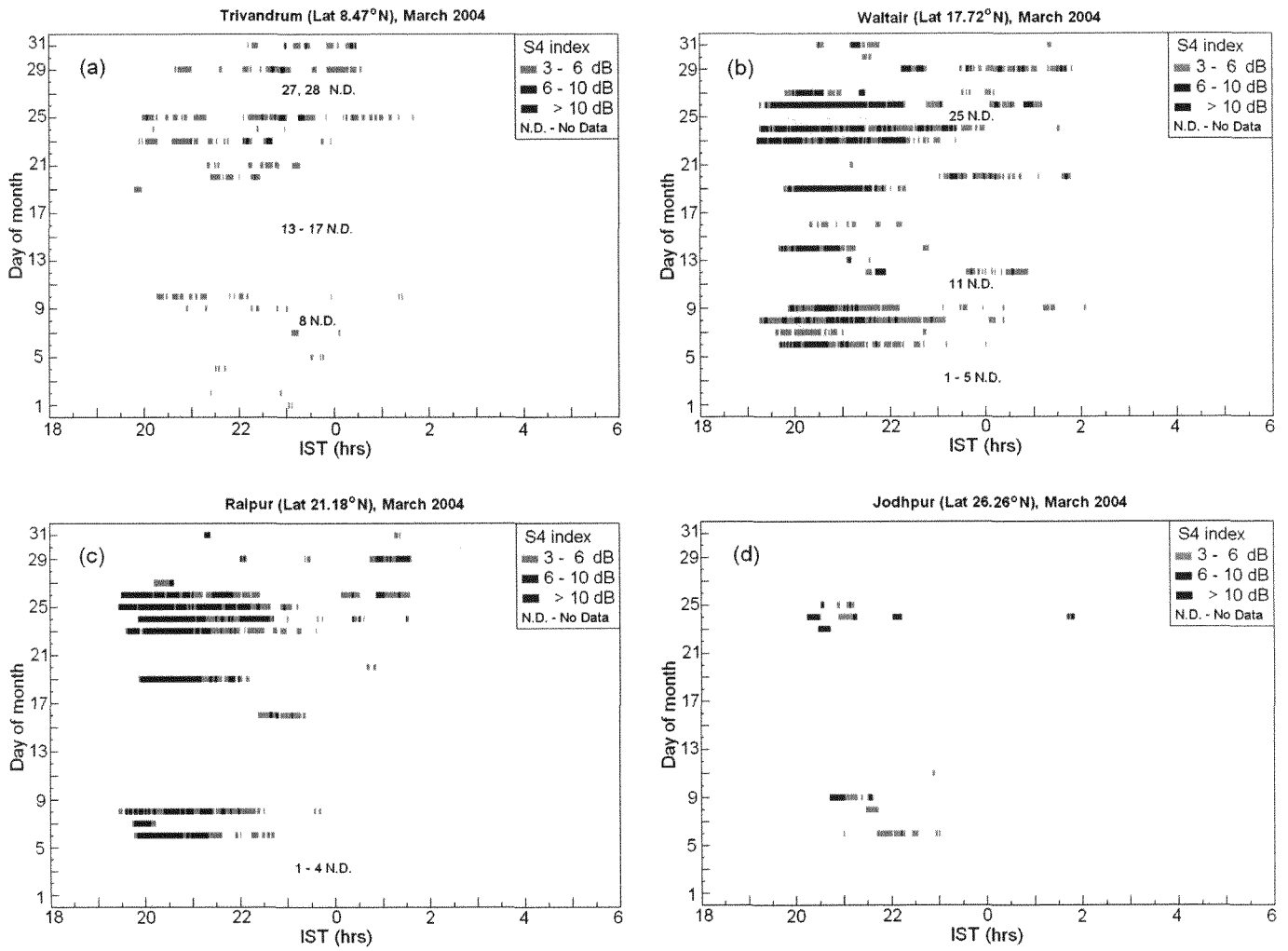
Figure 10 *Day to Day occurrence of scintillations at different power levels during the month of March 2004 at four typical Indian latitudes representing (a) Equatorial station (Trivandrum), (b) Low latitude station (Waltair), (c) Anomaly crest station (Raipur), (d) Station beyond the anomaly crest (Jodhpur)*
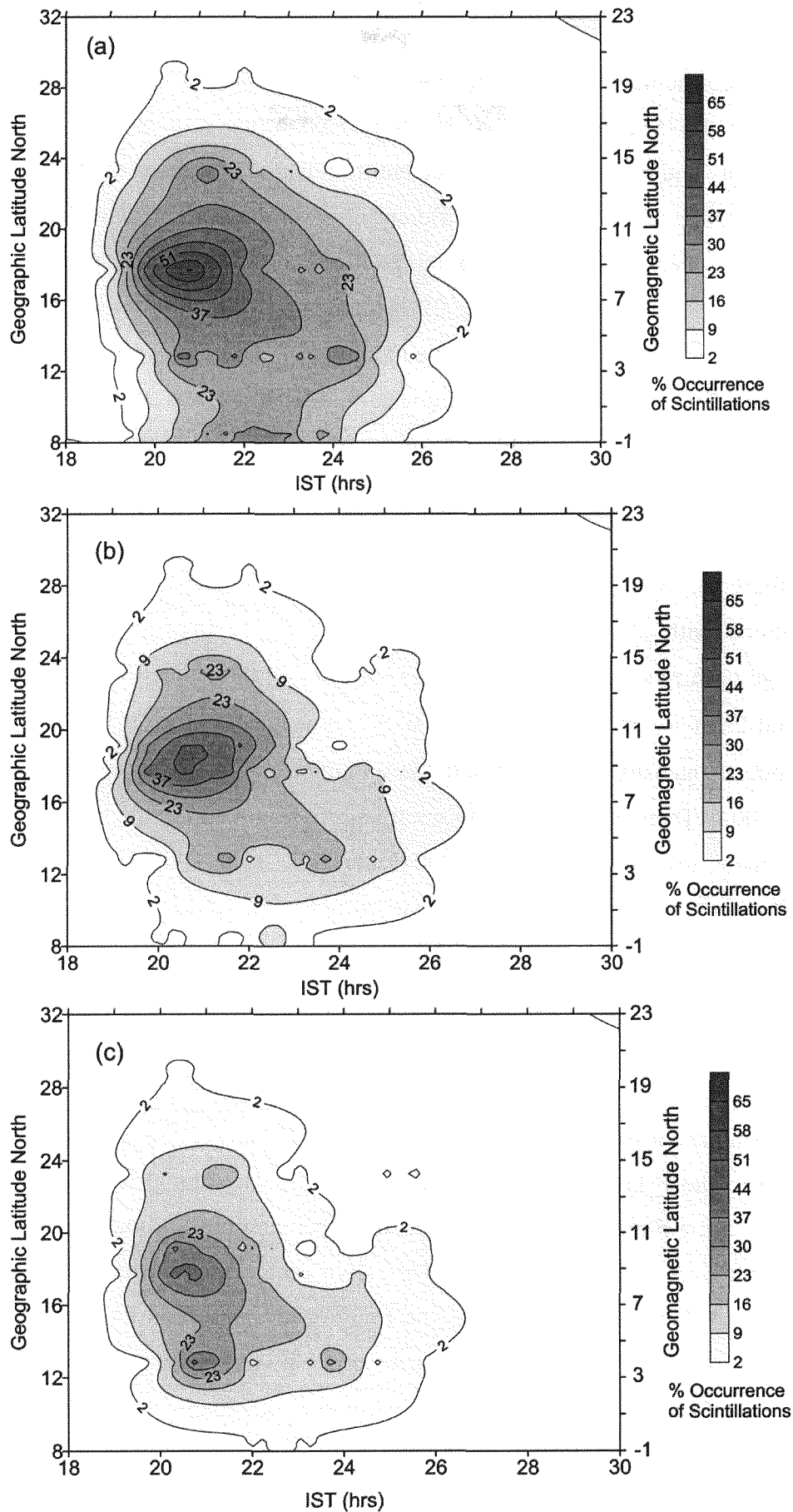
Figure 11. *Temporal and spatial variation of percentage occurrence of scintillation activity as a function of their intensity over all the Indian stations as observed from GPS S4 index data for the equinox month of March 2004 at power levels of (a) 3 to 6 dB (b) 6 to 10 dB and (c) >10 dB.*

17

The constellation of orbiting GPS satellites radiating signals at the L-band frequency of 1.575 GHz has given an unique opportunity to measure the S4-index simultaneously and continuously over the entire Indian region using the GPS network of receivers installed, almost evenly, at different places in India. The data of S4-index thus collected has been categorized into three different power levels, namely all those scintillations greater than 3 dB (S4 = 0.17), those greater than 6 dB (S4 = 0.3) and all those greater than 10 dB (S4 = 0.45). The monthly mean percentage occurrences of these scintillations for the 18 month period (January 2004 to July 2005) are computed, and their temporal (month to month) and spatial (latitudinal) variations are presented in Figs. 12 a, b & c respectively representing the three different power levels. It is strikingly observed from this figure that the occurrence of scintillations is maximum during the equinox months. From Fig. 12(a) which corresponds to the occurrence of scintillations with all power levels > 3dB, it may be noticed that the maximum percentage occurrence is seen around the vernal equinox months of March and April of 2004, and February and March of 2005 at all latitudes upto 20° N. The next maximum with reduced intensity occurs around the autumn equinox months of September and October 2004. There is practically no scintillation activity during the winter and summer months of the low sunspot years of 2004 and 2005 at the L-band frequency of 1.575 GHz. The equinoxial maxima are explained on the basis of the alignment of the solar terminator with the magnetic meridian in both the hemispheres (Tsunoda, 1985). Over the sunlit hemisphere, the E-region ionization short circuits the polarization electric fields, developed in the F-region during the evolution phase of the ESF irregularities. During the equinox, the solar terminator aligns closely with magnetic meridian and thereby simultaneously decreasing the conductivity of the E-regions that are magnetically conjugate to the F layer, through which currents flowing along the geomagnetic field lines connect the F region to the E regions on either side of the equator (which acts as a short circuit over sunlit hemisphere). This alignment causes the decrease in E-region conductivity, which opens or releases the F region dynamo electric field which in turn produces the E x B upward drift of the equatorial F layer, creating favorable conditions for the generation of plasma irregularities during the equinox months as seen above.
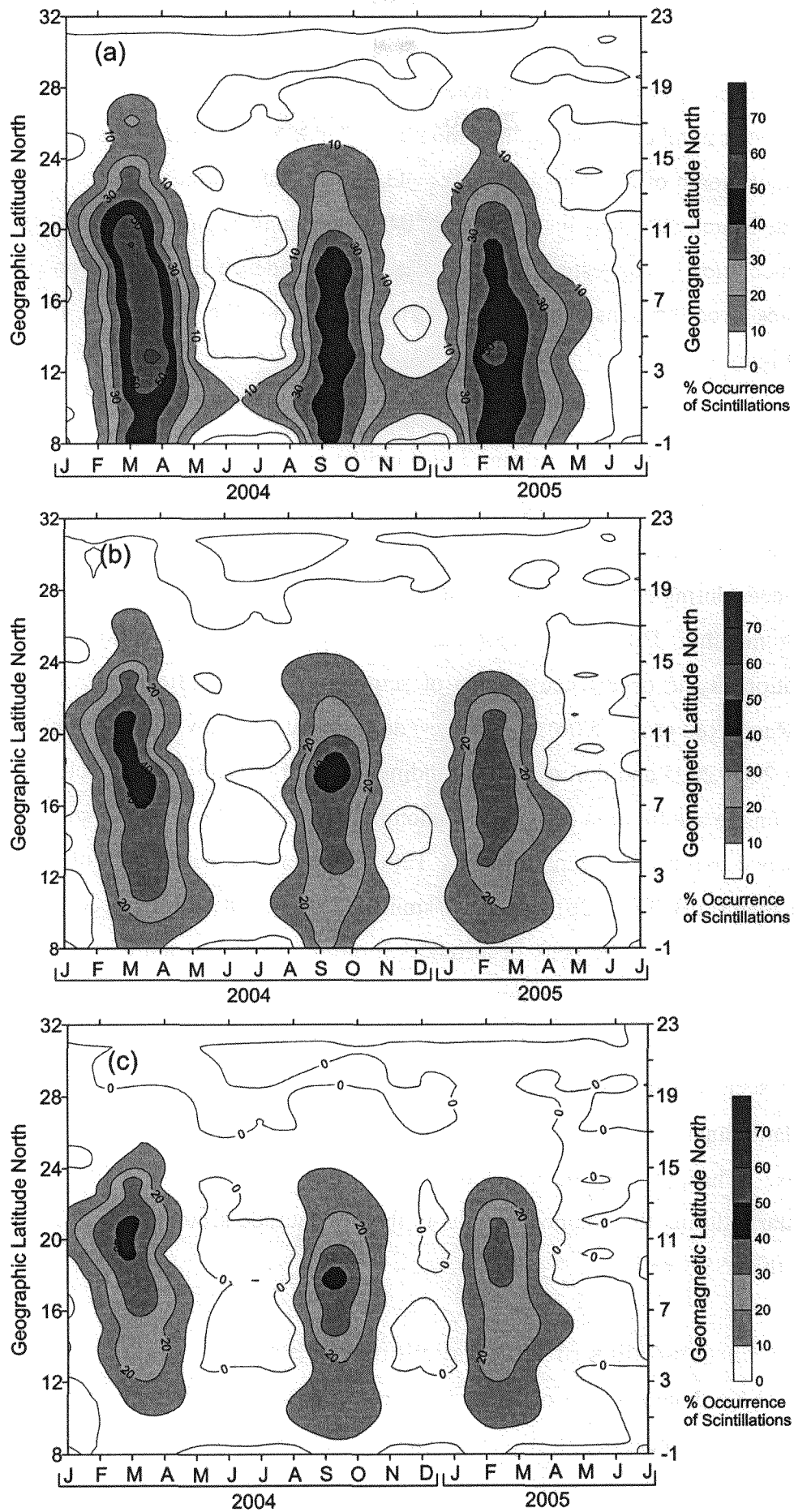
Figure 12. *Temporal & Spatial variation in the Occurrence of scintillations during the low sunspot activity years of 2004 and 2005 at different power levels of (a) >3 dB, (b) >6 dB, (c) >10 dB.*

Further, it is interesting to note from Fig.12 (a) that, even though the monthly mean sunspot number of the equinox month of March '05 (Rz = 24.8) is lower than that of a winter month of November '04 (Rz = 43.7), the scintillation activity is much higher (45%) in March '05 than in November '04 where there is practically no scintillation occurrence, clearly suggesting that the seasonal dependence of scintillation occurrence dominates over the sunspot number dependency during the descending phase of the sunspot number.

It is known that the occurrence of scintillations in the equatorial regions increases with the increase of sunspot activity maximizing during the HSSA period. Also, the occurrence of scintillations is modulated by the seasonal effect with maximum occurrences during equinox months followed by winter and minimum occurrence during summer months. During the moderate to high sunspot activity periods, the seasonal modulation in the occurrence pattern of scintillations is significant (DasGupta et al., 1983; Rama Rao et al., 2006). However, during relatively low sunspot number periods such as 2004-2005 and during the descending phase of the sunspot number, the seasonal control on the scintillation activity is predominantly perceptible over the sunspot number dependence as may be seen from Fig. 12(a). Further, the occurrence of scintillations greater than 6 dB (Fig. 12b) also show similar features, but with reduced percentage of occurrences and with the peak occurrences limiting to reduced latitudinal width. When we look at the percentage occurrence of scintillations greater than 10 dB (Fig.12c), which are of serious concern in trans-ionospheric communication at the L-band frequencies, it may be seen that the occurrences are relatively reduced and are mostly confined to a lesser latitudinal belt around 20° N during the vernal equinox and to 18° N in the autumn equinox. Thus, it may be concluded that strong (>10 dB) scintillations do occur, particularly during the equinox months in the low latitude sectors such as in India even during the LSSA period.

2.3b   Characteristics of TEC depletions/bubbles

The ordinary source of equatorial electrodynamics is the thermospheric dynamo that powers the equatorial electrojet (Haerendel and Eccles, 1992; Eccles, 1998). During the daytime, at ionospheric F- region altitudes the vertical polarization electric fields setup by the dynamo currents that are created by thermospheric winds, are short circuited through the conducting sunlit E-layer to the north and south of the magnetic equator.

However, after sunset, the eastward electric field attributed to the F-region dynamo is enhanced following the decrease in the E region conductivity, this field induces the upward E x B drift. This pre-reversal enhancement of the eastward electric field raises the F-layer at the magnetic equator to high altitudes, where the recombination rates are low and the conditions are favorable for generation of instabilities on the bottomside of the F-layer. Also sharp upward density gradients are developed after sunset due to the rapid recombination of electrons and ions. The nonlinear development of these instabilities leads to the formation of the plasma depleted bubbles (Woodman and La Hoz, 1976; Kelley, 1989). The polarization electric field within the bubbles is higher, as a result, the bubbles rise to the topside at a velocity higher than the ambient plasma drift (Anderson and Haerendal, 1979). The steep gradients on the edges of the depletions generate the small scale irregularities as the bubbles rise to great heights (Costa and Kelley, 1978), these are widely recognized as plumes on radar backscatter maps (Woodman and La Hoz, 1976) extending along the magnetic field line to the anomaly crests of about $\pm$ 15° magnetic latitudes. In the present study, the scintillations observed with the GPS L-band frequency of 1.575 GHz, around the anomaly crest regions are often found to be associated with the plasma bubbles, which are detected as TEC depletions in the GPS TEC data.

It is known that the occurrence characteristics of the plasma depletions depend strongly on season and longitude (Aarons, 1993; Huang et al., 2001). When the depleted ionospheric plasma comes into the line-of-sight between the GPS satellite and the receiver, the TEC decreases and is observed as depletion in the diurnal variation of TEC. It is also found that the presence of TEC depletions are often accompanied by amplitude scintillation of high intensity and fading rates, particularly, during the pre-midnight period where there may be a series of bubbles occurring within a single scintillation patch. Similar features in the occurrence of bubbles and scintillations are also reported by Yeh et al., (1979), Dasgupta et al., (1983).

Plasma depletions are of particular importance when they extend to the latitudes of the anomaly crest region; where these bubbles intersect the highest levels of electron density, so that transionospheric radio frequency propagation through this intersection undergoes the highest disruptive levels of scintillation, both in amplitude and in phase levels which are the highest during solar maximum (Klobuchar et al., 1991). In the present study, several depletions in TEC are detected which are often accompanied by the

presence of intense scintillations as seen from the increase in the S4 index measured by the GPS L1 signal. This can be seen from the typical examples of depletions in TEC, shown in Fig. 13. It is observed that when the plasma depletion is detected in the vertical TEC data derived from the satellite pass, the spatial gradients of TEC (ΔTEC/ΔLatitude, ratio of change in TEC to the change in latitude) at the edge of the bubbles are found to vary from 10 to 40. These density gradients give rise to favorable conditions for the generation of small scale irregularities that effect the L-band frequencies. However, in the present study strong scintillations (S4 $\geq$ 0.45 $\approx$ 10 dB) are found to occur at and around the equatorial ionization anomaly region if the gradients are greater than 15. Further, these gradients are found to vary from 15 to 40 closer ($\pm$ 5°) to the anomaly crest region. As the plasma depletions extend in latitude to the crest regions, the strong scintillations which are associated with small scale irregularities contribute for degradation of the positional accuracies in the Satellite Navigational systems such as GPS. In Figs. 14 a & b, are shown typical example, in the nocturnal occurrence pattern of depletions and associated scintillations (S4 index), respectively, as a function of latitude in the Indian region for the month of March 2004. The S4 index and the TEC depletions detected from the GPS signals are plotted in these figures spatially, where the blue circles in Fig. 14(a) indicate the plasma depletions, and the red circles show loss of lock events in the phase channel of the GPS receiver that are discussed in the later section of this paper
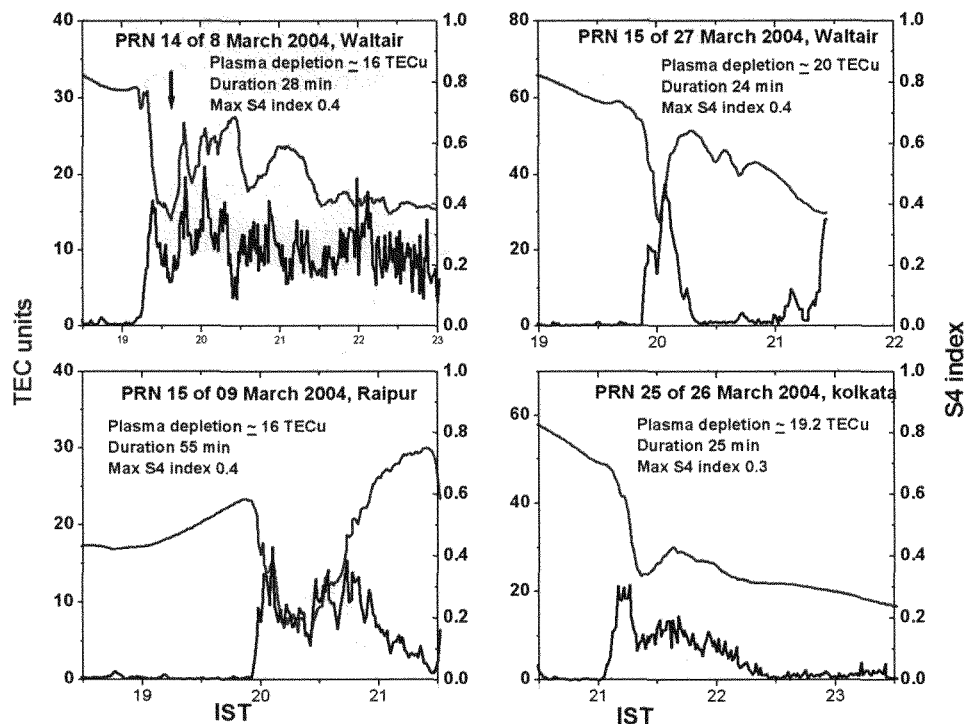
Figure 13. *Some examples of scintillations (S4 index) associated with TEC depletions observed in the GPS data at four typical Indian stations.*

22

It may be seen from Fig 14(a) that most of the depletions seen are confined to the anomaly crest region of geomagnetic latitudes ranging from 5° to 15° N (i.e., 15° to 25° N geographic latitudes). The same belt of latitudes also show the presence of intense (S4 index >0.45) scintillation activity as may be seen from Fig. 14b. The scintillations are moderate to weak at latitudes closer to the equator because of the presence of low electron density and absence of the short scale length irregularities, which do not significantly affect the radio signals at L-band frequencies. Whereas at the anomaly crest region, because of increased electron densities and the presence of large gradients, the generation of small scale irregularities is relatively high which contribute to the occurrence of strong scintillations that severely effect the L-band signals.
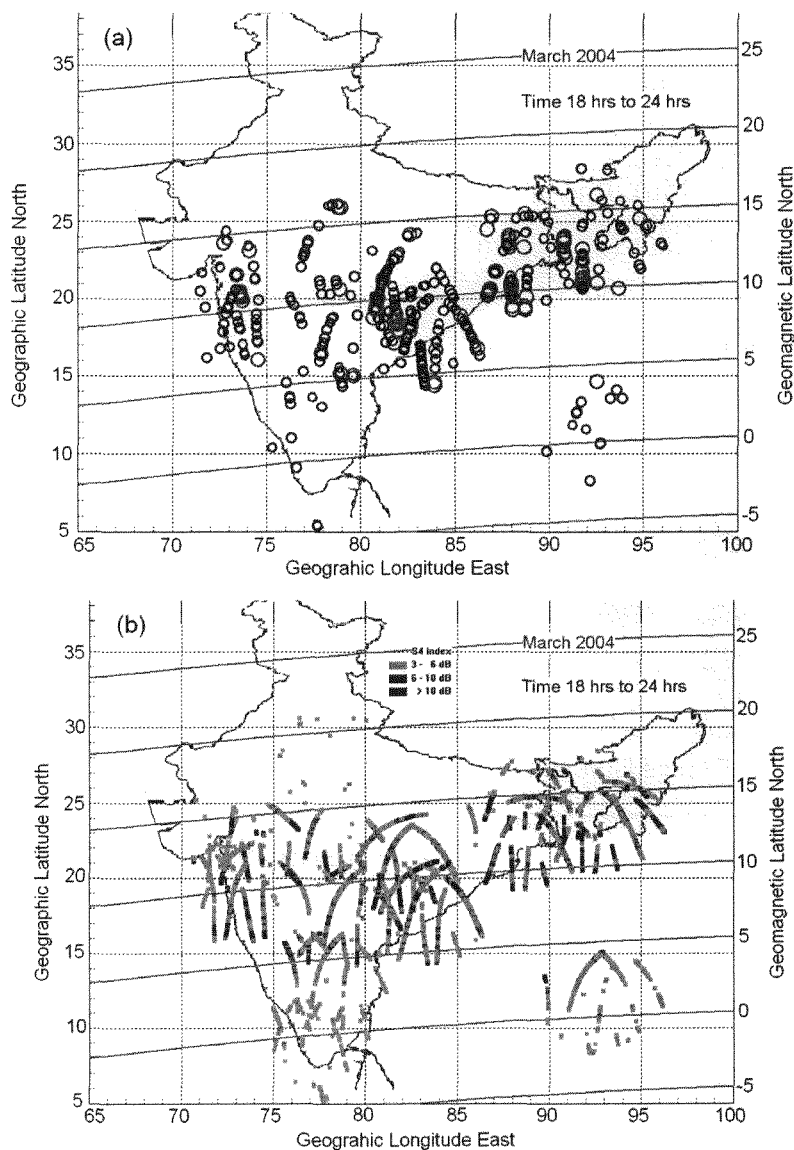
Figure 14. *Occurrence of L-band scintillations associated with TEC depletions (bubbles) and loss of lock events during the month of March 2004.*
(a) Bubbles (blue circles) and loss of locks of the GPS receivers (red circles) and
(b) The scintillations at three different power ranges of 3 to 6 dB (Green), 6 to 10 dB (Blue) and > 10 dB (Red).

It is also interesting to note that the TEC depletions and the strong scintillation events are aligned more to the geomagnetic latitudes showing the geomagnetic field control on these events. The population of scintillation events of high S4 index is more in the inner edge of the anomaly crest compared to that at the outer edge where the TEC falls of sharply towards the mid latitudes than towards the equator. The length of durations of the plasma depletions and the depth of their amplitudes determine the effect on the GPS based navigation systems. In the equinox month of March 2004 alone, a maximum number (297) of depletions are detected from all the Indian stations. The TEC depletions observed during this month are categorized into different ranges of durations and amplitudes in TEC units, and presented as histograms in Figs. 15(a) & (b) respectively. It is observed from these histograms that the most probable bubble durations vary from 5 to 25 minutes (Fig 15a) and the most probable depth of depletions vary from 5 to 15 TEC units (Fig. 15b). It is known that the ionosphere causes a group delay of 0.162 meters per one TEC unit (10^{16} ele/m^2) at the GPS L1 frequency of 1.575 GHz (Warnant, 1997; Klobuchar et al., 1993), and thus in the present case the depletion amplitudes of 5 to 15 TEC units introduce range errors of the order of 1 to 3 metres.
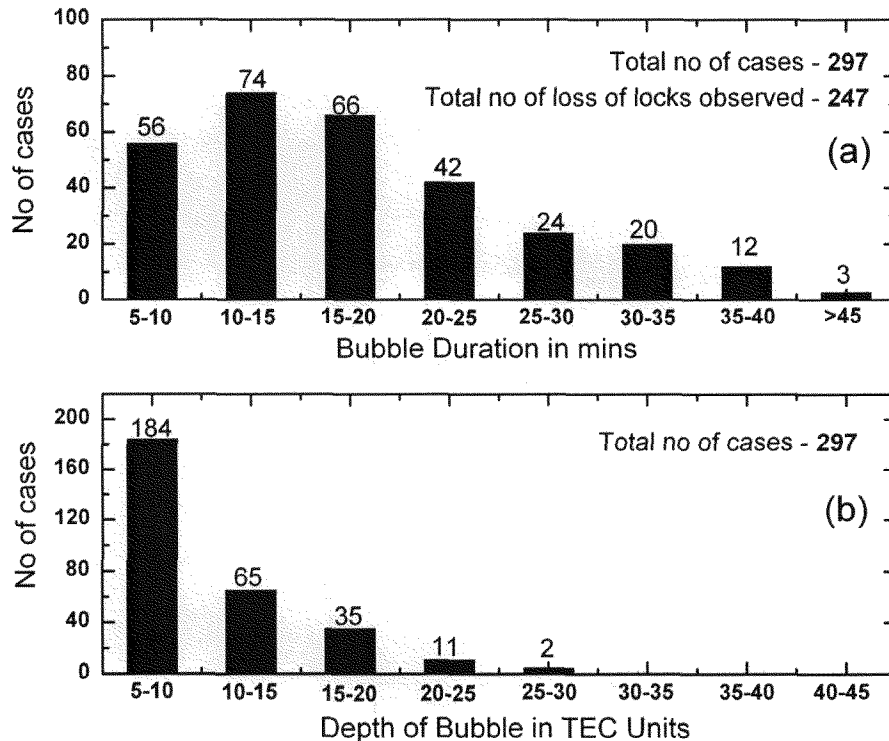
Figure 15. *Histograms showing the duration (a) and intensity (b) of the TEC depletions observed over Indian region for the month of March 2004.*

In Table 1, is listed the number of depletion events observed from all the 18 Indian stations in each month during the 18 month period from January 2004 to July 2005. It can be seen from the table that a total number of 971 depletion events are detected over the entire Indian region during the 18 month period. Further, it may also be seen that maximum number of depletions occur in the equinox months of March, April, September and October of 2004, and February & March of 2005, and at stations in the geographic latitude range of 13° to 24° N. Also, it is seen from the table that the latitude range in the occurrence of depletions is slightly higher in the vernal equinox months of March & April, compared to the autumnal equinox months of September & October 2004. Further, the occurrence of depletions during February & March of 2005 is smaller compared to those during the corresponding months of the year 2004 owing to the decrease in the monthly average sunspot number (Rz) from 49 in March 2004 to 25 in March 2005.

Station Geographic Latitude	Number of **depletions** observed for the months during Jan 2004 to Jul 2005																		
Months with Rz	Jan 37.3	Feb 45.8	Mar 49.1	Apr 39.3	May 41.5	Jun 43.2	Jul 51.1	Aug 40.9	Sep 27.7	Oct 48.0	Nov 43.5	Dec 17.9	Jan 31.3	Feb 29.2	Mar 24.5	Apr 24.4	May 42.6	Jun 39.6	Jul 39.9
8.47	--	0	1	10	0	0	0	0	5	2	0	0	0	3	0	0	0	0	0
10.83	--	--	--	--	--	--	--	--	10	4	1	0	0	8	14	0	0	0	0
11.67	--	--	10	17	0	0	--	2	3	--	--	--	--	--	6	3	1	0	0
12.95	0	1	8	21	0	0	0	0	29	19	0	1	0	15	8	2	0	0	0
17.44	--	--	32	9	0	0	0	0	37	35	0	0	0	28	15	2	0	0	0
17.72	--	--	55	15	0	0	0	3	20	20	0	2	0	30	8	0	0	0	0
19.09	--	--	43	6	0	0	0	0	22	17	0	0	2	23	7	1	2	0	0
21.18	--	--	39	5	0	0	1	0	16	16	0	0	0	21	7	0	0	0	0
22.64	0	2	45	4	0	0	0	0	23	2	0	0	0	11	3	0	0	0	0
23.06	--	0	10	0	0	0	0	0	0	7	0	0	0	8	1	0	0	0	0
23.28	0	1	12	0	0	0	0	0	7	5	0	0	0	2	1	0	0	0	0
23.83	--	3	31	2	0	0	4	1	4	2	0	0	0	12	2	0	0	0	0
26.12	0	0	5	0	0	0	0	0	0	0	0	0	0	3	0	0	0	0	0
26.26	0	2	1	0	0	0	0	0	0	0	0	0	0	0	0	0	0	0	0
26.68	--	0	5	0	0	0	3	0	1	0	0	0	0	0	0	0	0	0	0
26.76	--	--	0	0	0	0	0	0	0	0	0	0	0	0	0	0	0	0	0
28.58	2	0	0	0	0	0	0	0	0	0	0	0	0	0	0	0	0	0	0
31.09	--	--	--	--	--	0	0	0	0	0	0	0	0	0	0	0	0	0	0
Total no of depletions	2	9	297	89	0	0	8	6	177	129	1	3	2	164	72	8	3	0	0

Table 1. *Number of depletions observed from each station (latitudes of each station tabulated) for every month during the period from January 2004 to February 2005. The monthly mean sunspot numbers are also shown under each of the months.*

Further, at the anomaly crest region, during the post sunset hours when strong scintillation (S4 > 0.45) activity is present, the TEC has shown presence of strong depletions with amplitudes varying from 10 to 30 TEC units which correspond to a range error of 1.62 to 4.87 meters in the GPS positional accuracies. Hence, the duration of the depletion and depth of amplitude in TEC play an important role in introducing errors in the range correction to be made in SBAS signals derived from the reference stations. Therefore, the region of geographic latitude range of $15°$ to $25°$ N in the Indian sector, which is almost 50% of the SBAS area in India is expected to be frequently affected by strong scintillations and depletions, particularly during equinox months even during the LSSA periods (2004-2005). The range of latitudes or the FIR region that is likely to be affected by the scintillations could be expected to increase significantly with the increase of the solar activity.

2.3c   Loss of lock of the GPS receivers

GPS receiver tracking performance gets degraded in the presence of scintillation effects. Rapid phase variations cause a doppler shift in the GPS signal, which may exceed the bandwidth of the phase lock loop (PLL), resulting in a loss of phase lock (Leick, 1995). Additionally, amplitude fades can cause the signal-to-noise-ratio (SNR) to drop below the receiver threshold level, resulting in loss of code lock. These effects have a larger impact on tracking loops employing codeless and semicodeless technologies, versus full code correlation. In particular, codeless and semicodeless tracking loops experience losses of 27–30 dB and 14–17 dB respectively, with respect to full code correlation, and are therefore more susceptible to the effects of amplitude fading (Leick, 1995). The L2 phase locked loop (PLL) also employs a narrower bandwidth (≈ 1 Hz, compared to ≈ 15 Hz for L1) to eliminate excess noise, and is more susceptible to loss of lock due to phase scintillations. These effects therefore are of significant concern for users who require dual frequency data for estimation of ionospheric effects, or resolution of widelane ambiguities. Investigations of GPS receiver performance recently conducted by Knight et al. (1999) using an array of eight GPS receivers in the equatorial region have shown that on some occasions during which L2 phase observations were corrupted up to 27% of the time, and loss of L2 code lock was often observed. L1 tracking performance was degraded to a lesser extent. The results of such studies depend not only on the magnitude of scintillation activity, but also on the receiver tracking capabilities that can vary widely between different manufacturers and models.

In Fig. 16 is shown some typical samples of loss of locks detected in the GPS receiver TEC data during times of severe scintillations. It can be noticed from this figure that loss of locks are observed when ever the S4 index exceeds 10 dB (S4 > 0.45) power levels. The receiver PLL recovers from the loss of lock within a short duration of about 1 to 4 minutes. It was also observed that the receiver looses its lock more than once when the scintillation activity is severe particularly at the anomaly crest regions, and also if the satellite is at a low elevation angle.
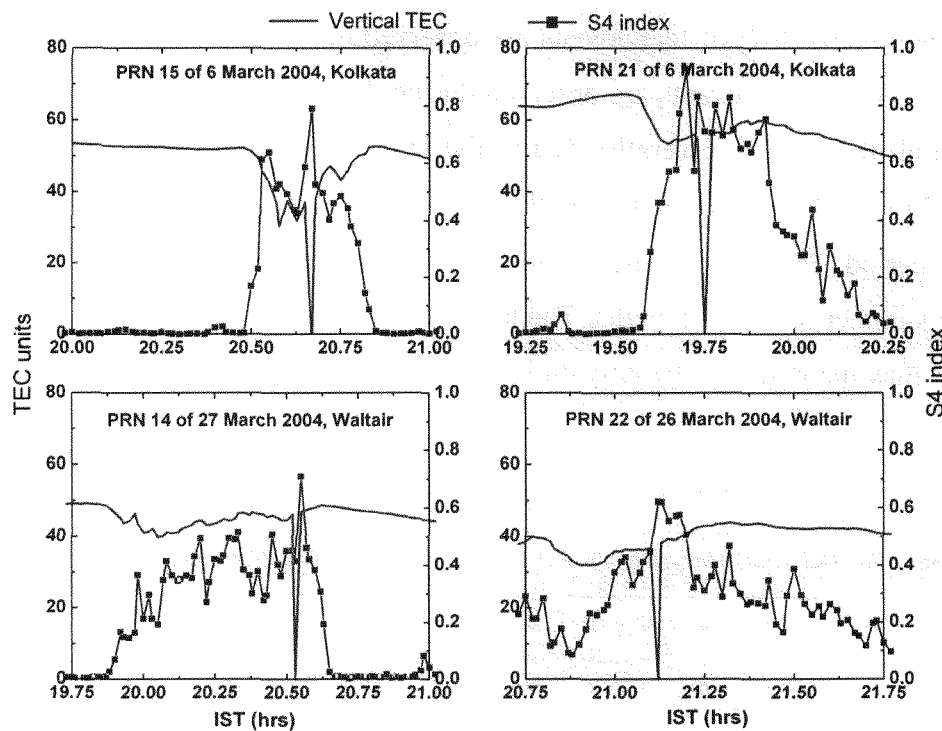
Figure 16. *Typical examples of scintillation activity showing the values of S4 index exceeding 0.45 causing loss of lock of the GPS receivers.*

It may be recalled that in Fig. 14(a), the spatial distribution in the occurrence of depletions/bubbles, where the loss of lock events (red circles) of the receivers are also plotted for examining the spatial distribution of these events during the typical month of March 2004. It may also be seen from this figure that the loss of locks occur in the same geographic latitude range of 15° to 25° N similar to those of bubbles and strong scintillations. Also as shown in Fig. 14(b), the corresponding S4 index data for the month of March 2004 shown as colour coded dots (red) for S4 index > 0.45, it is observed that there is a good correspondence between the occurrence of S4 index greater than 0.45 and the loss of lock events. From a close examination of the GPS data with the help of an in

house developed software, it is noticed that whenever the L-band scintillation activity (S4) exceeds 0.45 or 10 dB power levels, the receiver looses its lock for a duration of about 1 to 4 minutes. The GPS receiver loss of locks thus detected from all the Indian stations during each of the 18 months data are listed as a function of latitude in Table 2. From this table it is seen that the GPS receivers are subjected to loss of locks mostly during the equinox months of March, April, September and October of 2004, and February and March of 2005 where the S4 index often exceeded 0.45 (10 dB). Further, it may also be seen that these loss of locks occur in the regions of strong scintillation (10 dB and above) occurrences as may be seen from Fig. 12(c). During this period, maximum number of loss of lock events are observed only during equinox months. As many as 247 loss of lock events are observed during the month of March 2004 (Fig. 15) alone from all the GPS receivers located in the Indian region. The geographic latitude zone of 15° to 25° N is identified to be the most affected region in the equinox months during this period. There are practically no loss of lock events in the post midnight hours and during summer & winter months. The latitude range as well as the number of loss of lock events may increase significantly during the ascending phase of the sunspot activity.

Station Geographic Latitude	Number of **Loss of locks** observed for the months during Jan 2004 to Jul 2005																		
Months with Rz	Jan 37.3	Feb 45.8	Mar 49.1	Apr 39.3	May 41.5	Jun 43.2	Jul 51.1	Aug 40.9	Sep 27.7	Oct 48.0	Nov 43.5	Dec 17.9	Jan 31.3	Feb 29.2	Mar 24.5	Apr 24.4	May 42.6	Jun 39.6	Jul 39.9
8.47	0	0	1	10	0	0	0	0	5	2	0	0	0	3	0	0	0	0	0
10.83	--	--	--	--	--	--	--	--	10	4	0	0	0	8	14	0	0	0	0
11.67	--	--	10	17	0	0	0	2	3	--	--	--	--	--	6	0	0	0	0
12.95	0	0	8	21	0	0	0	0	29	19	0	0	0	15	8	0	0	0	0
17.44	--	--	32	9	0	0	0	0	37	35	0	0	0	28	15	0	0	0	0
17.72	--	--	55	15	0	0	0	3	22	20	0	0	0	30	8	0	0	0	0
19.09	--	--	43	6	0	0	0	0	20	17	0	0	0	23	7	0	0	0	0
21.18	--	--	39	5	0	0	1	0	16	16	0	0	0	21	7	0	0	0	0
22.64	0	1	45	4	0	0	0	0	23	2	0	0	0	11	3	0	0	0	0
23.06	--	0	10	0	0	0	0	0	0	7	0	0	0	8	1	0	0	0	0
23.28	0	1	12	0	0	0	0	0	7	5	0	0	0	2	1	0	0	0	0
23.83	--	2	31	2	0	0	0	1	4	2	0	0	0	12	2	0	0	0	0
26.12	0	1	5	0	0	0	0	0	0	0	0	0	0	3	0	0	0	0	0
26.26	0	1	1	0	0	0	0	0	0	0	0	0	0	0	0	0	0	0	0
26.68	--	0	5	0	0	0	0	0	1	0	0	0	0	0	0	0	0	0	0
26.76	--	0	0	0	0	0	0	0	0	0	0	0	0	0	0	0	0	0	0
28.58	1	0	0	0	0	0	0	0	0	0	0	0	0	0	0	0	0	0	0
31.09	--	0	0	0	0	0	0	0	0	0	0	0	0	0	0	0	0	0	0
Total loss of locks	1	6	195	30	0	0	1	0	65	39	0	0	0	36	22	0	0	0	0

Table 2. *Number of loss of lock events observed from each station (latitudes of each station tabulated) for every month during the period from January 2004 to February 2005. The monthly mean sunspot numbers are also shown under each of the months.*

The plasma depletions that might have been detected simultaneously by two or three GPS satellite signals that have the line of sight through the same depletion region are not separately accounted for in this preliminary study, as the emphasis is on the number of available satellite PRNs that are effected by these plasma depletions for SBAS operation. Therefore, the number of TEC depletions detected here may give rise to a larger number than the actual number of plasma bubbles that existed in that region at that point of time, and each of the detected bubble may have different durations and magnitudes depending on their intersection direction and duration with that particular plasma depletion. This may be one of the reasons for the number of TEC depletions observed are much greater (971) than the number of loss of lock events (345) detected. Further all the plasma depletions may not intersect high density TEC regions to have enough gradients on the edges of the depleted regions that can generate the small scale length irregularities to produce intense scintillations (> 10 dB), which can lower the GPS signal power below the threshold level (due to strong amplitude scintillation) or can cause rapid phase changes in the received signal that results in loss of lock of the receiver. Further, no loss of lock events are detected without the presence of TEC depletion and intense scintillation activity (S4 >0.45).

2.4 Summary of results and discussion

The scintillation index (S4) data at the L-band frequency of 1.575 GHz recorded simultaneously from the GPS receivers installed at 18 different locations (nearly at a spacing of 5° x 5° grid) under ISRO-GAGAN programme in the Indian region has given an unique opportunity, for the first time, to study the spatio-temporal and intensity characteristics of the ionospheric scintillations during the 18 month period from January 2004 to July 2005.

The results of the study reveal the following characteristic features in the occurrence of the L-band scintillations in the Indian equatorial and low latitude region.

I   L-band scintillation characteristics

(1) The percentage occurrence of L-band scintillations is maximum during the post sunset to midnight hours with very little activity during the post midnight hours in the current LSSA period of 2004-2005.

(2) The percentage occurrence of weak (3 to 6 dB) scintillations is maximum at the equatorial region owing to the presence of low ambient electron densities and low

gradients accompanied by the presence of large scale length irregularities at the equator during the LSSA conditions in the years 2004 & 2005.

(3) The intensity of scintillation (S4 index) is maximum (>10 dB) around the anomaly crest region because of the presence of high electron densities and large gradients accompanied by the presence of small scale irregularities at the anomaly crest regions.

(4) Scintillations are found to occur mostly during the equinox months with practically no activity during summer and winter months of the LSSA period of 2004-2005.

(5) The occurrence of strong scintillations is mostly confined to 15° to 25° N geographic latitudes i.e., 5° to 15° N geomagnetic latitudes in the Indian region.

(6) It is found that the equinoxial feature dominates in the occurrence of scintillations giving rise to higher occurrences in the equinox months of March, April of 2004 & 2005 with practically no activity during winter and summer months.

II Characteristics of electron density depletions/bubbles observed in the GPS TEC data

(1) Significant number of TEC depletions are found to occur during the post sunset hours, often accompanied by the occurrence of scintillations at the L-band frequency of 1.575 GHz of the GPS L1 signal.

(2) The occurrence of these bubbles is also found to be maximum during the equinox months peaking around the equatorial ionization anomaly crest region of 15° to 25° geographic latitudes.

(3) The most probable bubble durations vary from 5 to 25 minutes and their amplitudes vary from 5 to 15 TEC units that correspond to a range error of about 1 to 3 metres in the GPS navigation.

III Loss of lock of GPS receivers

(1) During the equinox months when the occurrence of strong scintillation is maximum (i.e. S4 > 0.45) around the EIA crest region, it is often found that the GPS receiver losses its lock for a short duration of 1 to 4 minutes in the phase channel (L1).

(2) Multiple number of loss of locks are also observed during times of some strong scintillation events.

(3) During the entire period of 18 months of data considered in the present study, a total of 395 loss of lock events are detected in the Indian sector which are of serious concern for the GPS navigation.

(4) The bubble events, as well as the loss of lock events are likely to increase significantly during the high sunspot activity periods resulting in severe degradation in the trans-ionospheric communications and GPS navigation systems.

2.5 References

Aarons, J., Whitney, H. E., MacKenzie, E., and Basu, S.: Microwave equatorial scintillation intensity during solar maximum, Radio Sci., 16, 939–945, 1981.

Aarons, J.: Global morphology of ionospheric scintillation, Proc. IEEE, 70, 360-378, 1982.

Aarons, J.: The longitudinal morphology of equatorial F-layer irregularities relevant to their occurrence, Space Sci. Rev., 63, 209-243, 1993.

Anderson, D.N., and Haerendel, G.: The motion of depleted plasma regions in the equatorial ionosphere, J. Geophys. Res., 84, 4 251 - 4 256, 1979.

Basu, S., Kudeki, E., Basu, Su., et al.: Scintillations, plasma drifts, and neutral winds in the equatorial ionosphere after sunset, J. Geophys. Res., 101, 26 795-26 809, 1996.

Basu, S., MacKenzie, E., and Basu, Su.: Ionospheric Constraints on VHF/UHF Communications Links During Solar Maximum and Minimum Periods, Radio Science, 23, 363 - 378, 1988.

Conker, R.S., El-Arini, M.B., Hegarty, C.J., and Hsiao, T.: Modeling the effects of ionospheric scintillation on GPS/Satellite Based Augmentation System Availability, Radio Science, 38, doi: 10.1029/2000RS002604, 1 - 23, 2003.

Costa, E., and Kelley, M.C.: On the role of steepened structures and drift waves in equatorial spread F, J. Geophys. Res., 83, 4 359 - 4 364, 1978.

DasGupta, A., Aarons, Basu, S., J., Klobuchar, J. A., Basu, Su., and Bushby, A.: VHF amplitude scintillations and associated electron content depletions as observed at Arequipa, Peru, J. Atmos. Terr. Phys., 45, 15 - 26, 1983.

Doherty, P.H., Susan, H.D., and Valladares, C.E.: Ionospheric scintillation effects on GPS in the equatorial and Auroral regions, Journal of the Institute of Navigation, Vol. 50, No. 4, pp. 235-245, 2004.

Eccles, J. V.: Modeling investigation of the evening prereversal enhancement of the zonal electric field in the equatorial ionosphere, J. Geophys. Res., 103, 26 709, 1998.

Fejer, B .G., Scherliess, L., and de Paula, E. R.: Effects of the vertical plasma drift velocity on the generation and evolution of equatorial spread F, J. Geophys. Res., 104, 19 859 - 19 869, 1999.

Haerendel, G., and Eccles, J.V.: The role of the equatorial electrojet in the evening ionosphere, J. Geophys. Res., 97, 1 181, 1992.

Huang, C. Y., Burke, W. J., Machuzak, J. S., Gentile, L. C., and Sultan, P. J.: DMSP observations of equatorial plasma bubbles in the topside ionosphere near solar maximum, J. Geophys. Res., 106, 8 131 - 8 142, 2001.

Huang, C.S., and Kelly, M., C.: Nonlinear evolution of equatorial spread-F. Gravity wave seeding of Rayleigh Taylor instability, J. Geophys. Res., 101, 293 - 302, 1996.

Hysell, D. L. and Burcham, J. D.: JULIA radar studies of equatorial spread F, J. Geophys. Res., 103, 29 155 - 29 167, 1998.

Hysell, D.L.: An overview and synthesis of plasma irregularities in equatorial spread F, J. of Atmos. & Solar-Terrestrial Physics, 60, 1 037 - 1 056, 2000.

Kelley, M.C., LaBelle, J., Kudeki, E., Fejer, B.G., Basu, S., Basu, Su., Baker, K.D., Hanuise, C., Argo, P., Woodman, R.F., Swartz, W.E., Farley, D.T., and Meriwether, J.: The Condor equatorial spread F campaign: overview and results of the large scale measurements, J. Geophys. Res., 91, 5 487 - 5 503, 1986.

Kelley, M.C., Larson, M.F., LaHoz, C., and McClure, J.P.: Gravity wave initiation of equatorial spread-F: A case study, J. Geophys. Res., 86, 9 087 - 9 100, 1981.

Kelly, M.C., The earth's ionosphere, Academic Press, San Diego, 487, 1989.

Kintner, P.M., Kil, H., Beach, T.L., and de Paula, E. R.: Fading Timescales Associated with GPS signals and potential consequences, Radio Science, 36, 731 - 743, 2001.

Klobuchar, J. A., Anderson, D. N., and Doherty, P. H.: Model studies of the latitudinal extent of the equatorial anomaly during equinoctial conditions, Radio Science, 26, 1 025 - 1 047, 1991.

Klobuchar, J.A., Basu, S. and Doherty, P.: Potential limitations in making absolute ionospheric measurements using dual frequency radio waves from GPS satellites, Proc. of Ionospheric Effects Symposium, IES-93, May, 187 - 194, 1993.

Knight, M., and Finn, A.: The effects of ionospheric scintillation on GPS, Proceedings of

The institute of Navigation's ION GPS-98, Nashville, TN, September 15-18, 673 - 86, 1998.

Knight, M., Cervera, M., and Finn, A.: A comparison of predicted and measured GPS performance in an ionospheric scintillation environment, Proceedings of the ION GPS - 99, Nashville, Tennessee, September, 1999.

Leick, A.: GPS Satellite Surveying, second edition, JohnWiley & Sons, U.S.A., 1995.

Rama Rao, P.V.S., Tulasi Ram, S., Gopi Krishna, S., Niranjan, K., and Prasad D.S.V.V.D.: Morphological and Spectral Characteristics of L-band and VHF scintillations and their impact on trans-ionospheric communications, Journal of Earth Planets and Science, (in press), 2006.

Skone, S., and de Jong, M.: The impact of geomagnetic substorms on GPS receiver performance, Earth, Planetary and Space Sciences, 52, 1 067 - 1 071, 2000.

Tsunoda R. T.: Control of the seasonal and longitudinal occurrence of equatorial scintillations by longitudinal gradient in the integrated E-region Paderson conductivity, J. Geophys. Res., 90, 447 – 456, 1985.

Van Dierendonck, A.J., Fenton, P., and Klobuchar, J.: Commercial ionospheric scintillation monitoring receiver development and test results, Proceedings of the Institute of Navigation's 52nd Annual Technical Meeting, Cambridge, MA, 573 - 582, 1996.

Wanninger, L.: Effects of the Equatorial Ionosphere on GPS, GPS World, page 48. July 1993.

Warnant, R.: Reliability of the TEC computed using the GPS measurements: the problem of hardware biases, Acta Geodaetica et Geophysica Hungarica, 32(3-4), 451 - 459, 1997.

Woodman, R. F. and LaHoz, C.: Radar observations of F region equatorial irregularities, J. Geophys. Res., 81, 5 447 - 5 466, 1976.

Yeh, K. C., Liu, C. H., Soicher, H., and Bonelli, E.: Ionospheric bubbles observed by the Faraday rotation method at Natal, Brazil, Geophysical Research Letters, 6, 473 - 475, 1979.

3. Temporal and Spatial variations in TEC using simultaneous measurements from the Indian GPS network of receivers during the low solar activity period, 2004 - 2005

3.1 Introduction:

In the recent years, with the increasing demand on the trans-ionospheric communication systems used in the navigation of space borne vehicles such as satellites, aircrafts as well as surface transportation systems, the measurement of the true value of Total Electron Content (TEC) of the ionosphere has become important for making appropriate range corrections as well as in accounting for errors introduced in the range delays owing to the effects of space weather related events such as geomagnetic storms and scintillations due to ionospheric irregularities.

Broad features in the temporal and spatial behaviour of the total electron content of the ionosphere in the global perspective is fairly known to a great extent (Kane, 1980). The ionization in the equatorial and polar regions is known to be high compared to relatively moderate levels of electron content in the mid latitude ionospheric regions. Also the changes in the temporal and spatial features of TEC at the mid latitudes are relatively small compared to the equatorial and low latitude regions (Davies, 1980), where these changes are significant owing to the dynamical behaviour of the ionosphere because of the various processes associated with the phenomena of equatorial ionization anomaly (EIA) and equatorial spread-F (ESF) irregularities in these regions.

During the past three decades, with the availability of the orbiting satellites such as BE-B and BE-C, INTASAT and the geostationary satellites such as ATS-6, ETS-2 and SIRIO, several researchers have made significant contributions by making individual measurements of TEC from various locations in India (Rastogi and Sharma, 1971; Das Gupta and Basu, 1973; Rastogi et al., 1975; Rama Rao et al., 1977; Davies et al., 1979). The results of these studies have revealed the broad characteristic features in the morphological behaviour of the total electron content in the Indian sector. However, there were no coordinated, simultaneous and continuous measurements of TEC from all the latitude zones of the Indian region except for some measurements made with ATS-6 satellite when the satellite was housed at 35° E longitude during 1975-76 for SITE (Satellite Television Experiment) Experiment in India, where there were several data gaps during the late evening hours due to switching off of the beacons for saving power for the SITE programmes. Now, with the launching of the GAGAN project in India,

simultaneous and continuous measurements are being made for the past 3 years from the network of 18 dual frequency GPS receivers installed at (5° x 5° grid spacing) different latitude and longitude regions in the country. (http://www.aiaa.org/indiaus2004/Sat-navigation.pdf and http://www.mycoordinates.org/gagan-update-arjunsingh-mar-06.php). This network of GPS receivers has given an unique opportunity for a continuous monitoring of the behaviour of TEC in the entire Indian zone.

3.2 TEC measurement using Global Positioning System (GPS)

All modern TEC measuring techniques rely on the observation of signal phase differences or on pulse travel time measurements based on geostationary and orbiting satellite signals. A standard way of measuring TEC is to use ground-based receiver capable of processing signals from satellites in geostationary orbits and polar orbiting satellites. In the recent times, the Global Positioning System (GPS, or NAVSTAR), a satellite based navigation system is increasingly being used for all-weather precision navigation over land, sea and in air by both military and civilian users. In principle, it should be possible to get offset free TEC data from GPS by measuring the differential group delay instead of phase shift (or phase delay).

The dual frequency GPS receiver system provides a means of monitoring the effect of the ionosphere on GPS signals. It is particularly intended to measure the integrated ionization content between satellite and receiver, and is also capable of detecting scintillations at L-band frequencies. Operation at the L1 and L2 frequencies simultaneously permits measurement of the relative phase delay between the two signals, producing an unambiguous determination of the slant TEC, or the total number of electrons in a column of cross-sectional area of one square metre along the signal path between the satellite and the receiver. For a single frequency GPS receiver, ionospheric delay cannot be determined uniquely, but must be estimated from a model, with an uncertain effect on the final navigation solution. Thus, TEC is of significant concern for users of single frequency GPS receivers and particularly for those located under the equatorial ionization anomaly region, where the reliability of the GPS provided model is in question.

The GPS navigation system comprises of three distinct "segments" (Sonnenberg, 1988; Ackroyd and Lorimer, 1990), of which the first one is the space segment that consists of a constellation of 24 satellites transmitting coded signals downward to receivers on the Earth's surface. The second is the control segment that includes ground

stations used for monitoring satellites and sending upward signals for the engineering control of each satellite and its transmitted codes and waveforms. And the third one is the user segment which includes everyone with a GPS receiver who is making use of the transmitted signals. Satellites are equi-spaced around each of the six circular orbital planes inclined at 55° to the plane of the Earth's equator. The orbital altitude is $\approx$ 20,200 km, with an orbital period of 12 hours. The geometry in the location of the satellite constellation is such that, from any point on the Earth's surface with a reasonably unobstructed horizon, signals from at least four satellites will always be available in the line of sight and it will therefore be possible to solve for the four unknowns of the receiver, namely latitude, longitude, altitude and the combined satellite/receiver timing error.

Each satellite continuously transmits frequencies in the L-band of the microwave spectrum, at L1=1.57542 GHz and L2=1.2276 GHz respectively. The L1 and L2 carriers are phase coherent, both being derived from a common 10.23 MHz oscillator. Both the frequencies are modulated by a common binary code called precision code (P-code), the use of which allows the delay error introduced by ionospheric refraction to be eliminated from the final position determination, permitting the determination of the total electron content (TEC) along the signal path. This encrypted P-code is unavailable to the general user. The L1 frequency is also modulated by the coarse acquisition code (C/A code) and is used by single frequency receivers. The GPS receiver calculates its position by selecting the optimum configuration of four satellites and finding its range with respect to each satellite. The range is determined from the delay in the time taken for the signal to travel from each of the satellites to the receiver, as measured by the difference between the satellite transmit time, which is known, and the signal reception time which is measured by autocorrelation. However, this difference does not take into account any error in the receiver's clock relative to the satellite's clock and therefore the range is only approximate and is therefore called a pseudorange.

The ionosphere has a refractive index at radio frequencies, which is different from unity and can affect GPS signals in a number of ways as they pass from satellite to ground (Coco, 1991; Wanninger, 1993; Klobuchar, 1996). One of the significant effects is, the GPS signal traversing the ionosphere undergoes additional delay proportional to the total number of electrons in the cross-section volume measured in TEC units. The dual frequency GPS receivers use two frequencies L1 (1575.42 MHz) and L2 (1227.60

MHz) to compensate for the ionospheric delay, which remove these effects, at least to a first order approximation taking the advantage of the dispersive nature of the ionosphere, where the refractive index is a function of frequency. The ionospheric time delay at the L1 carrier frequency of f_1 as given by Klobuchar (1996) is

$$t_1 = 40.3 \times \left(\frac{TEC}{C \cdot f_1^2} \right) \qquad (3.1)$$

where C is the speed of light in free space. A dual frequency (f_1 and f_2) receiver measures the difference in time delay between the two frequencies, $\Delta t = t_2 - t_1$, given by

$$\Delta t = \left(\frac{40.3}{C} \right) \times \frac{TEC}{[(1/f_2^2) - (1/f_1^2)]} \qquad (3.2)$$

Thus, the time delay (Δt) measured between the L1 and L2 frequencies is used to calculate the TEC along the ray path. The calculation of TEC by the above method, using pseudorange data alone, can produce a noisy result, while the differential carrier phase gives a precise measure of relative TEC variations because the actual number of cycles of phase is not known. Absolute TEC cannot be obtained unless pseudorange is also used. Therefore, use of the pseudorange gives the absolute scale for TEC while differential phase increases measurement accuracy. Thus, the GPS data provides an efficient way to estimate TEC values with greater spatial and temporal coverage (Davies and Hartmann, 1997; Hocke and Pavelyev, 2001). Since the frequencies that are used in GPS system are sufficiently high, the signals are minimally affected by the ionospheric absorption and Earth's magnetic field, both in short-term as well as in long-term changes of the ionospheric structure.

In the Indian low latitude sector several isolated TEC measurements were made during the past three to four decades using data from a number of orbiting as well as geostationary satellite signals, the studies of which led to a broad understanding of the behaviour of the equatorial and low latitude ionosphere. However, in the recent past with the availability of simultaneous data of TEC from the Indian GPS network of receivers, it has become possible to make a simultaneous and systematic study on the behaviour of the ionosphere from a large and continuous database for use in the navigational application purposes over the Indian region.

The GPS has enormously increasing applications in Navigation, surveillance etc and recently in the Aircraft's landing category-I precision approach by augmenting the GPS with Space Based Augmentation System (SBAS) signal. Thus the TEC measurements have gained importance in estimating the range delays involved in the

GPS based navigation. Here we report the results obtained by the studies carried out using an 16 month TEC data from March 2004 to June 2005 recorded by the Indian GPS network of receivers.

3.3 Data and method of analysis

In the present study, the (slant) TEC data recorded at all the 18 different locations (Fig. 9) during the sixteen-month period from March 2004 to June 2005 is used in this analysis. Here, the slant TEC measurements made are the sum of the real slant TEC, the GPS satellite differential delay b_S (satellite bias) and the receiver differential delay, b_R (receiver bias). Therefore, the vertical TEC can be expressed as

$$VTEC = (STEC - [b_R + b_S])/S(E) \qquad (3.3)$$

where *STEC* is the slant TEC measured, *E* is the elevation angle of the satellite in degrees, *S(E)* is the obliquity factor with zenith angle *z* at the *Ionospheric Pierce Point* (IPP) and *VTEC* is the vertical TEC at the IPP. The obliquity factor, *S(E)* (or the mapping function) is defined as (Mannucci et al., 1993; Langley et al., 2002)

$$S(E) = \frac{1}{\cos(z)} = \left\{ 1 - \left(\frac{R_E \times \cos(E)}{R_E + h_S} \right)^2 \right\}^{-0.5} \qquad (3.4)$$

Where R_E is the mean radius of the Earth in km, h_S is the ionosphere (effective) height above the earth surface, *z* is the zenith angle and *E* is the elevation angle in degrees. The vertical TEC (*VTEC*) thus measured is used in deriving the results presented in the following sections of this paper.

3.4 Diurnal variation of Total electron content of the ionosphere in the Indian sector:

The slant TEC measured at every 1 min intervals from the data of GPS receivers are converted to vertical TEC for the study of temporal and spatial variations of TEC in the Indian region. In Figs. 17 (a), (b), (c) and (d), are presented the diurnal variation plots of TEC of a typical quiet day (2nd April, 2004) derived from all the visible satellites from four stations representing the four different latitude zones ranging from the equator to the ionization anomaly crest region and beyond namely, Trivandrum(8.5°N, 0° geomagnetic) an equatorial station, Waltair (17.7° N) a sub-tropical station, Kolkata (22.6° N) a station at the anomaly crest region and Delhi (28.6° N), a station located beyond the anomaly crest region. It may be seen from Fig. 17 [(a), (b), (c), and (d)] that there is a considerable spread in the diurnal variation of TEC derived from different satellite passes

visible at each of these four different stations. However, the spread in TEC at the equatorial station Trivandrum is minimum, whereas at Kolkata, the spread in TEC is maximum indicating the effect due to the presence of strong latitudinal gradients at the anomaly crest region compared to those at the equatorial station. Stations, Waltair and Delhi show spread of VTEC values as per the ionization distribution around their latitudes. In all these plots the diurnal variation shows a sharp and short lived day minimum ($\approx$5 TECU) in TEC occurring around 05 to 06 hrs IST (LT). A delayed (16 to 17 hrs IST) day maximum (55 TEC units) in TEC occurs at Trivandrum whereas at Kolkata a large (95 TEC units) and early (12 to 14 hrs IST) day maximum in TEC occurs. The corresponding diurnal variation in the range corrections to be made at the L1 frequency of 1.575 GHz vary from 1 to 10 meters at the equatorial station and from 1 to 16 meters at the anomaly crest station, on this particular day indicating that, different regions in India need different range corrections to be made in the navigational applications.
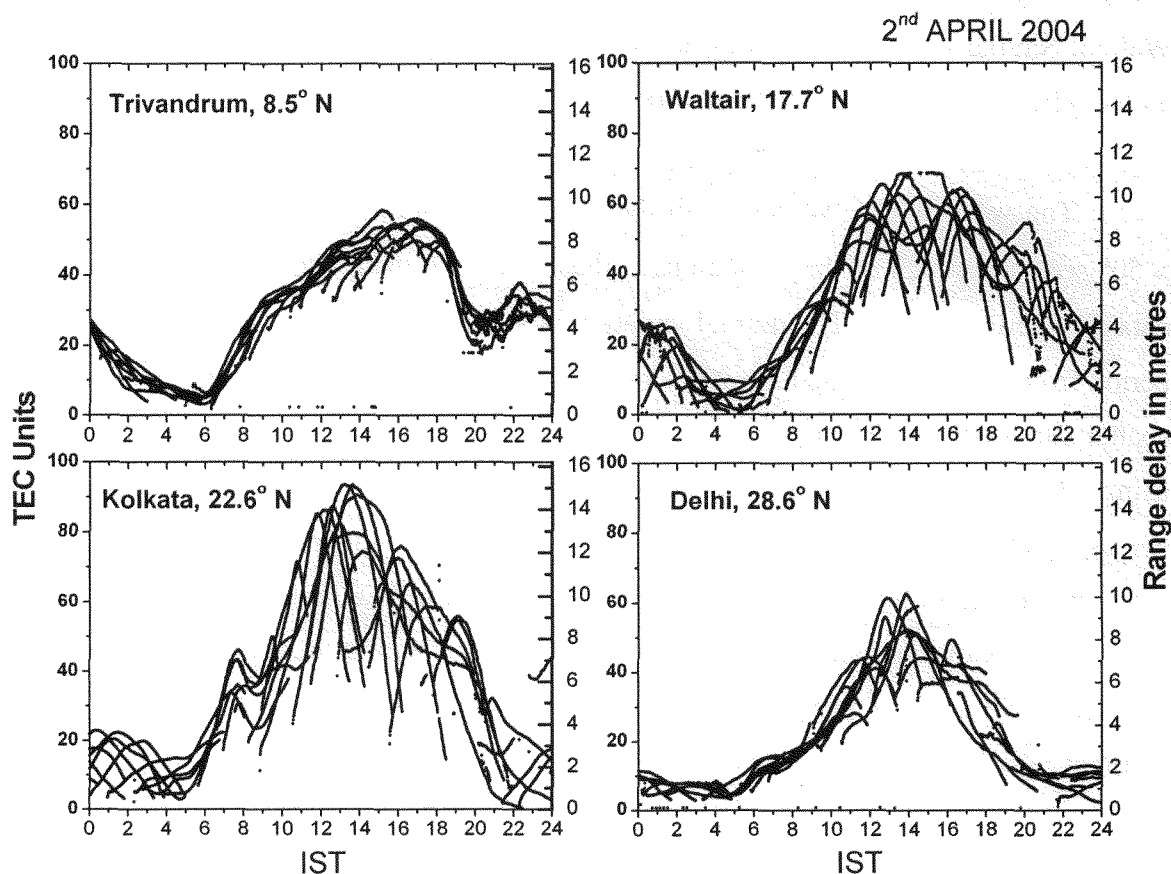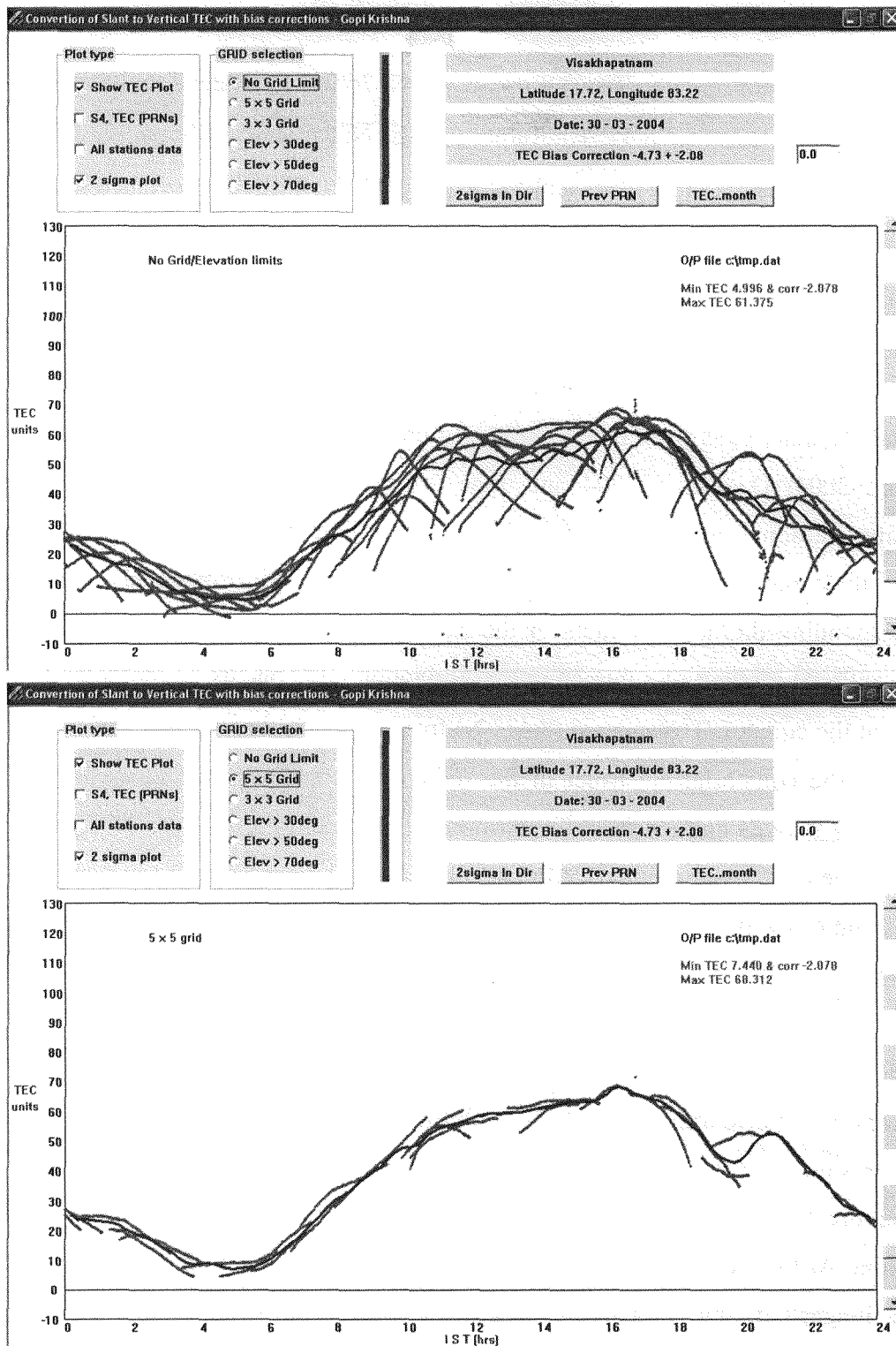

Fig. 17   *The diurnal variation of vertical TEC/range delays measured using GPS receivers from four different stations near the equator (Trivandrum), the low latitude (Waltair), the anomaly crest region (Kolkata) and beyond the crest region (Delhi).*

Fig. 18(a) shows a plot of the diurnal variation of TEC over a low latitude station, Waltair (17.7° N, 83.3° E) derived from all the visible satellite passes, on a typical quiet day, 30th March 2004 (a quiet day as per the classification given in the webpage http://swdcwww.kugi.kyoto-u.ac.jp/qddays/index.html). It is observed from this figure that the diurnal variation of the TEC measured from different passes vary (spread) significantly owing to the spatial and temporal variations in TEC, because these values are derived from different GPS satellite passes that are spread in different parts of the sky and at different local times over Waltair region. After making a number of trial runs, to obtain a good average diurnal variation plot of TEC, an elevation mask angle of 50° is arrived at to be ideally suited to eliminate the low elevation angle effects due to multipath and tropo-scatter due to water vapor on the measured TEC values. In Fig. 18 (b) is shown the diurnal variation of the vertical TEC thus derived from Waltair for passes with elevation angles > 50°. This TEC data is then subjected to a two-sigma (2σ) iteration, and the resulting values represent the average diurnal variation of TEC on that day over Waltair. Similar procedure is followed in computing the diurnal variations of TEC over all the other stations in the entire network.

The vertical TEC values of all the visible satellite passes with elevation angles > 50° seen from each of the 18 stations is thus computed using the measured slant TEC data as described above. The diurnal variation plots for each of the days of the 16 month period from March 2004 to June 2005 are prepared for a detailed study of temporal and spatial variations of TEC over the Indian region using a Software developed in house using VC++ for this purpose. The red curves in Figs. 18 (a) and (b), show the iterated average plots of the vertical TEC thus derived using this software. The biases of the receiver are determined by observing the day minimum TEC values from the diurnal variation plots of the respective stations and then by subjecting them to 2 sigma iterated average of all satellite passes at each of the stations. This process is also carried out automatically by the above software.

Fig. 18 *Diurnal Variation of Vertical TEC with time at Visakhapatnam for a typical day of 30th March 2004, subjected to two sigma iteration (red line) and automatic calculation of receiver bias using the software developed.*
(a) without any elevation mask angle and
(b) with an elevation mask angle of $50° ≈ 5° × 5°$ grid.

For making a appropriate and systematic study on the latitudinal behavior of the diurnal variation of TEC, in the Indian sector, the GPS-TEC data from a total of seven

41

different locations namely, Trivandrum (8.47° N, 76.91° E), Bangalore (12.95° N, 77.68° E), Hyderabad (17.44°, 78.47° E), Raipur (21.18° N, 81.74° E), Bhopal (23.28° N, 77.34° E), Delhi (28.58° N, 77.21° E) and Shimla (31.09° N, 77.07° E) situated approximately along the common meridian of 77° E longitude, extending all the way from the magnetic equator (Trivandrum) to the equatorial ionization anomaly crest region (Raipur and Bhopal) and beyond (Delhi and Shimla) are considered. The vertical TEC derived from the measured GPS slant TEC (as described in the previous section) has been computed for all the quiet days from the seven identified stations for three typical months namely, March 2004, December 2004 and June 2004 representing the equinox, winter and summer seasons respectively. Mass plots of the diurnal variations of TEC for each of these three months are presented in Figs. 19, 20 and 21 respectively along with the corresponding diurnal variations of the equatorial electrojet strengths derived from the conventional method of subtracting the horizontal components of the earths's magnetic field at the equator, Trivandrum (8.47° N) from that at Alibagh (18.5° N), a station lying outside the equatorial electrojet in the Indian region (Chandra and Rastogi, 1974). In general it may be noticed from these figures that the diurnal maxima of TEC are highest during the equinoxial month of March followed by the winter month, December. During the summer month of June the diurnal maxima are minimum. In the equinoxial month of March (Fig. 19) it may also be noticed that the diurnal minimum in TEC occurs around 05:00 to 06:00 hrs LT in the equatorial ionization anomaly zone i.e., from Trivandrum to Raipur. Whereas, beyond the anomaly crest region i.e., at Delhi and Shimla, the day minimum is flat during most of the nighttime hours (22:00 to 06:00 hrs LT), a feature that is similar to that at mid-latitudes. Secondly, the early morning increase in TEC is relatively fast at Trivandrum, Hyderabad and Raipur compared to that at Delhi and Shimla. At the equatorial station, Trivandrum, the day maximum is relatively broad and is of longer duration compared to that at the anomaly crest regions, Raipur and Bhopal. In particular, during the month of March the late afternoon decrease in TEC is equally steeper with occasional post sunset enhancements around the anomaly crest region encompassing stations like Hyderabad, Raipur and Bhopal. During the equinoxial month of March there is a nighttime maintenance of ionosphere with an average TEC value of about 15 to 20 TEC units in the diurnal variations at stations up to the anomaly crest region even during this low sunspot activity period (2004-2005). During the winter month of December also similar features are seen but with reduced intensity.
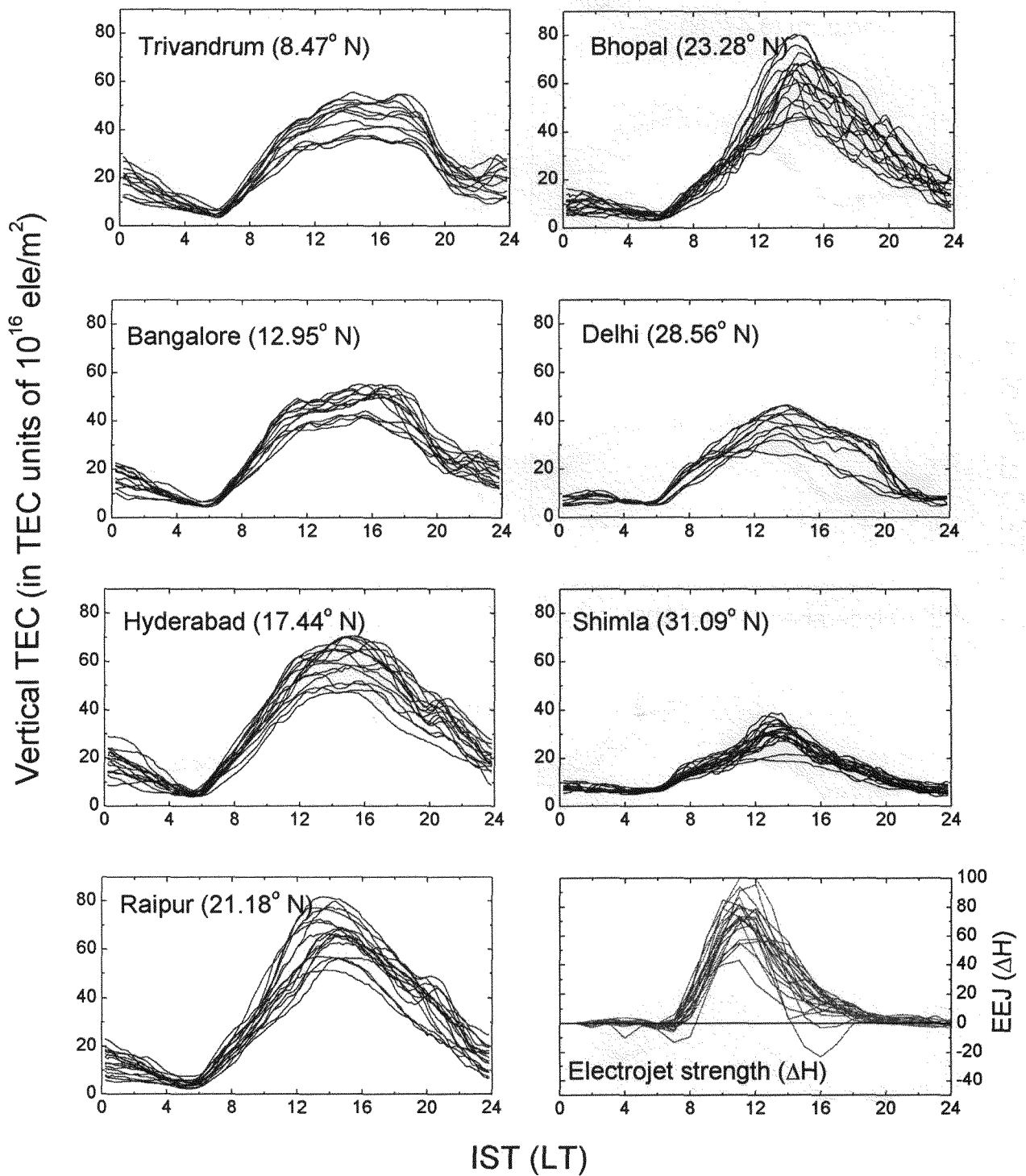
March 2004

Fig. 19   *Mass plots of the diurnal variation of TEC measured at seven locations situated along a common meridian of 77° E longitude for the quiet days in the equinoxial month of March 2004 presented along with the diurnal variations of the corresponding electrojet strength (EEJ) variations.*
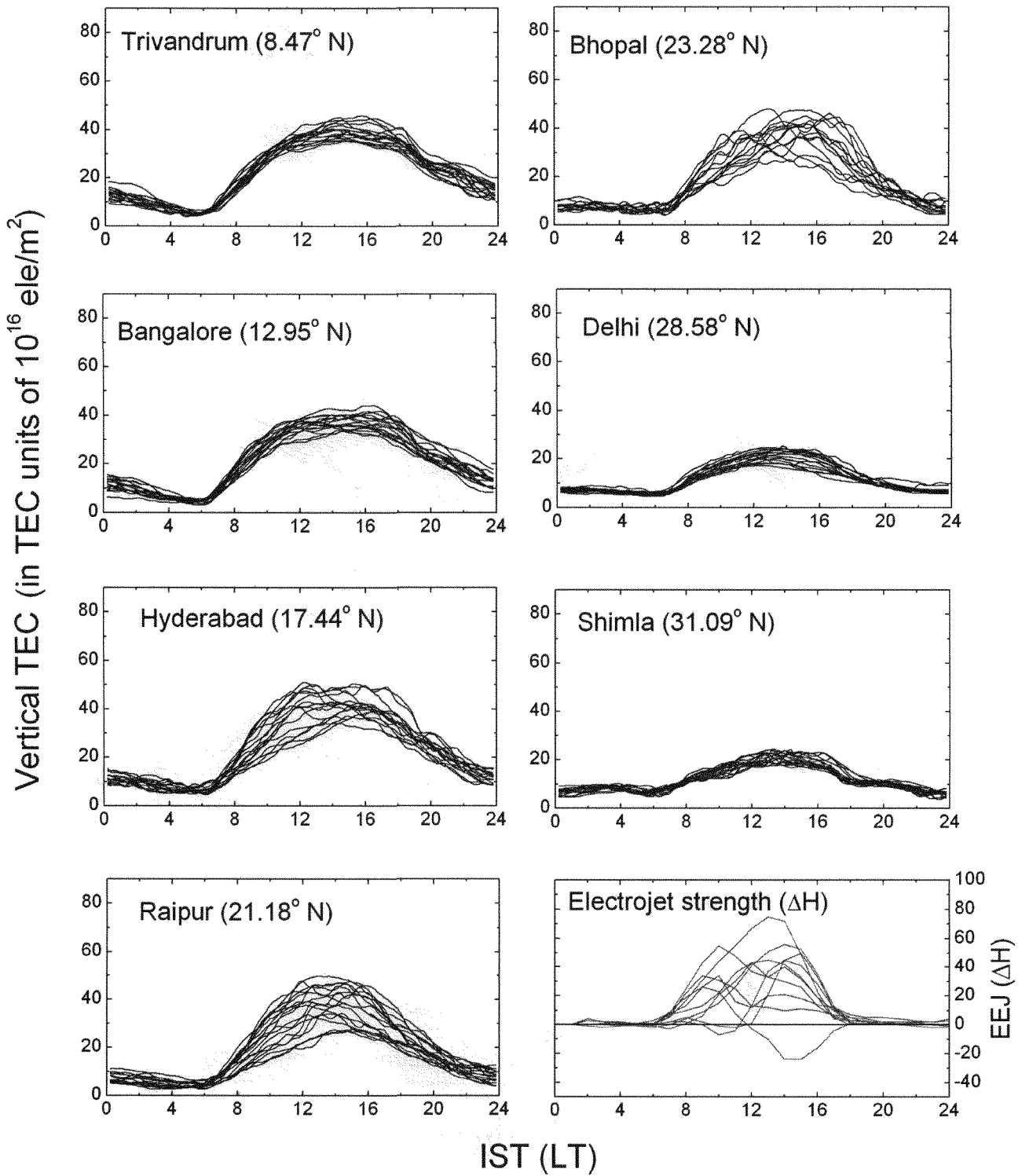
December 2004

Fig. 20 *Mass plots of the diurnal variation of TEC measured at seven locations situated along a common meridian of 77° E longitude for the quiet days in the winter month of December 2004 presented along with the diurnal variations of the corresponding electrojet strength (EEJ) variations.*
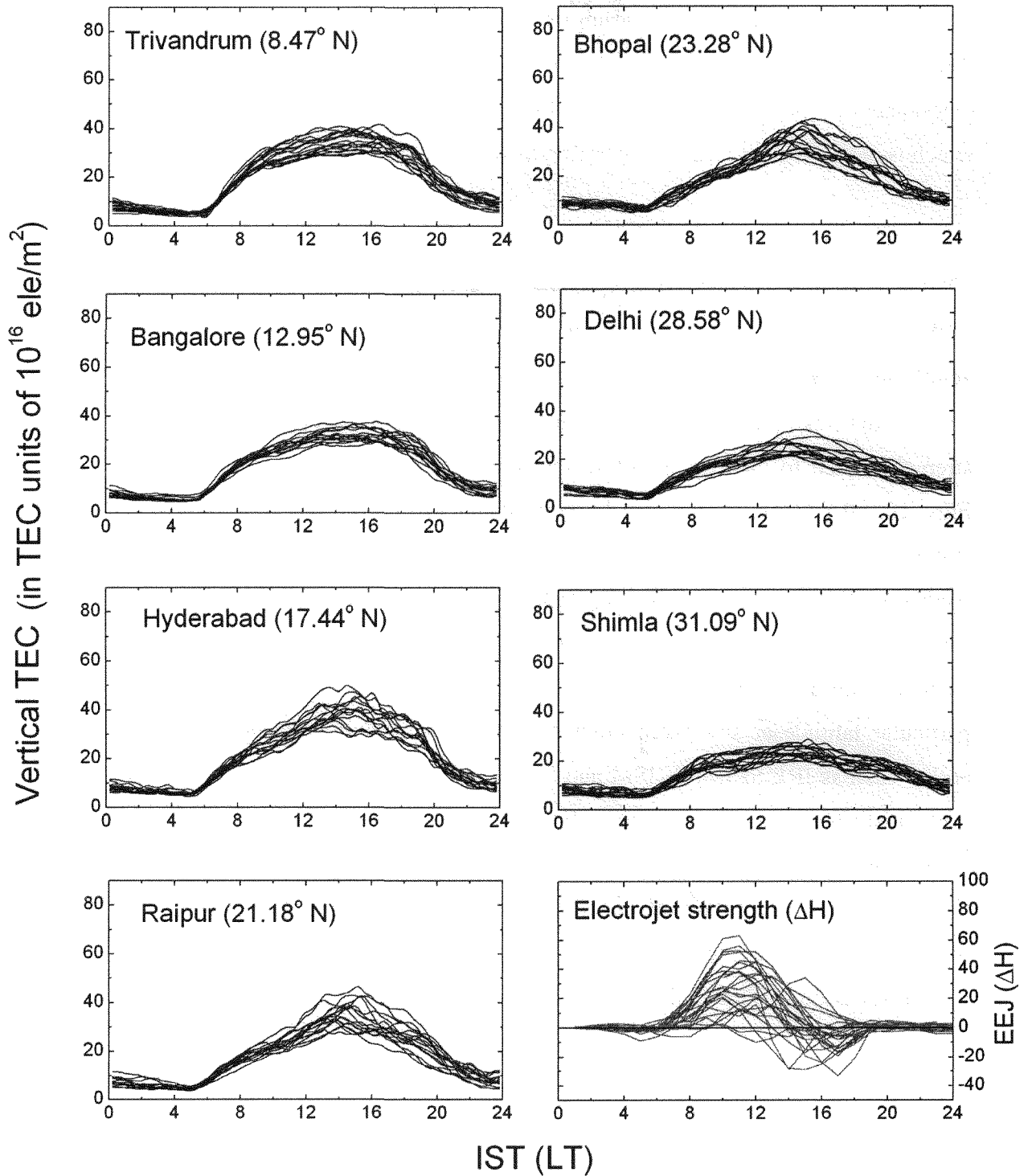
June 2004

Fig. 21 *Mass plots of the diurnal variation of TEC measured at seven locations situated along a common meridian of 77° E longitude for the quiet days in the summer month of June 2004 presented along with the diurnal variations of the corresponding electrojet strength (EEJ) variations.*

Whereas during the summer month of June, the night time values of TEC are almost constant at the minimum level during most of the night time hours. In all these figures (Figs. 19, 20 and 21), one very important feature that is noticeable is the day to day randomness in the variation of TEC particularly, during the mid day to pre-dawn hours, which is of serious concern in forecasting as well as in navigation.

This randomness in the day to day variation in TEC (Kane, 1980; Mendillo et al., 1980 and Modi & Iyer, 1989) may be attributed to the changes in the activity of the sun itself and to the associated changes in the intensity of the incoming radiations, and the zenith angle (χ) at which they impinge on the earth's atmosphere, in addition to the changes that take place in the earth's magnetic field and the equatorial electrojet (EEJ) strength, added to the effects due to the dynamics of the neutral winds. Further, from Figs. 19, 20 and 21, it may also be noticed that the day to day variability in the EEJ strength is equally significant to that of the TEC during all the three months considered. Added to all these, the plasma flow associated with the EIA may also play a significant role in the day to day variability of the observed diurnal variations in TEC at different stations in the Indian region. Therefore, forecasting TEC of the Indian ionosphere at any particular latitude at any given point of time is a difficult task, and the models used earlier such as IRI, SLIM, PRISM and SUPIM from different groups world over did not give satisfactory results that agree with the measurements made in the equatorial and low latitude regions. Therefore, there is an absolute need to develop a model that is suitable to the Indian equatorial and anomaly crest regions, taking into account the various mechanisms and parameters that play a major role in introducing randomness in the diurnal variation of TEC in the Indian region.

3.5 Seasonal variation in TEC

Following the procedure described in Section-4 the data of the diurnal variation of the 16 month period i.e., from March 2004 to June 2005 is considered for computation of the diurnal variation of TEC during all the quite days. The contour diagrams of the average diurnal variation of the electron content for each of the 16 months at each of the local hours at Trivandrum, Hyderabad, Raipur and Delhi representing the four different latitude zones in the Indian sector are presented in Fig. 22(a, b, c and d) respectively. It may be seen from these figures that the diurnal maximum in TEC occurs approximately between 12:00 to 16:00 hrs LT particularly at Hyderabad, Raipur and Delhi, whereas at

the equatorial station Trivandrum, the occurrence of the diurnal maximum is slightly delayed and occurs around 16:00 hrs LT. The highest day maximum TEC ($\approx$ 60 TEC units) occurs at Raipur and Hyderabad peaking around the equinoxial months of September, October and the winter month of November, while at Delhi a reduced diurnal maximum ($\approx$ 40 TEC units) occurs during the same months. At all these four stations the equinoxial maxima showing the semi-diurnal variation in TEC is strongly evident indicating the role played by the solar zenith angle variation in the changes produced by the level of production of ionization, added to the role played by the equatorial ionization anomaly and the strength of the equatorial electrojet, which also maximize during the equinoxial months.
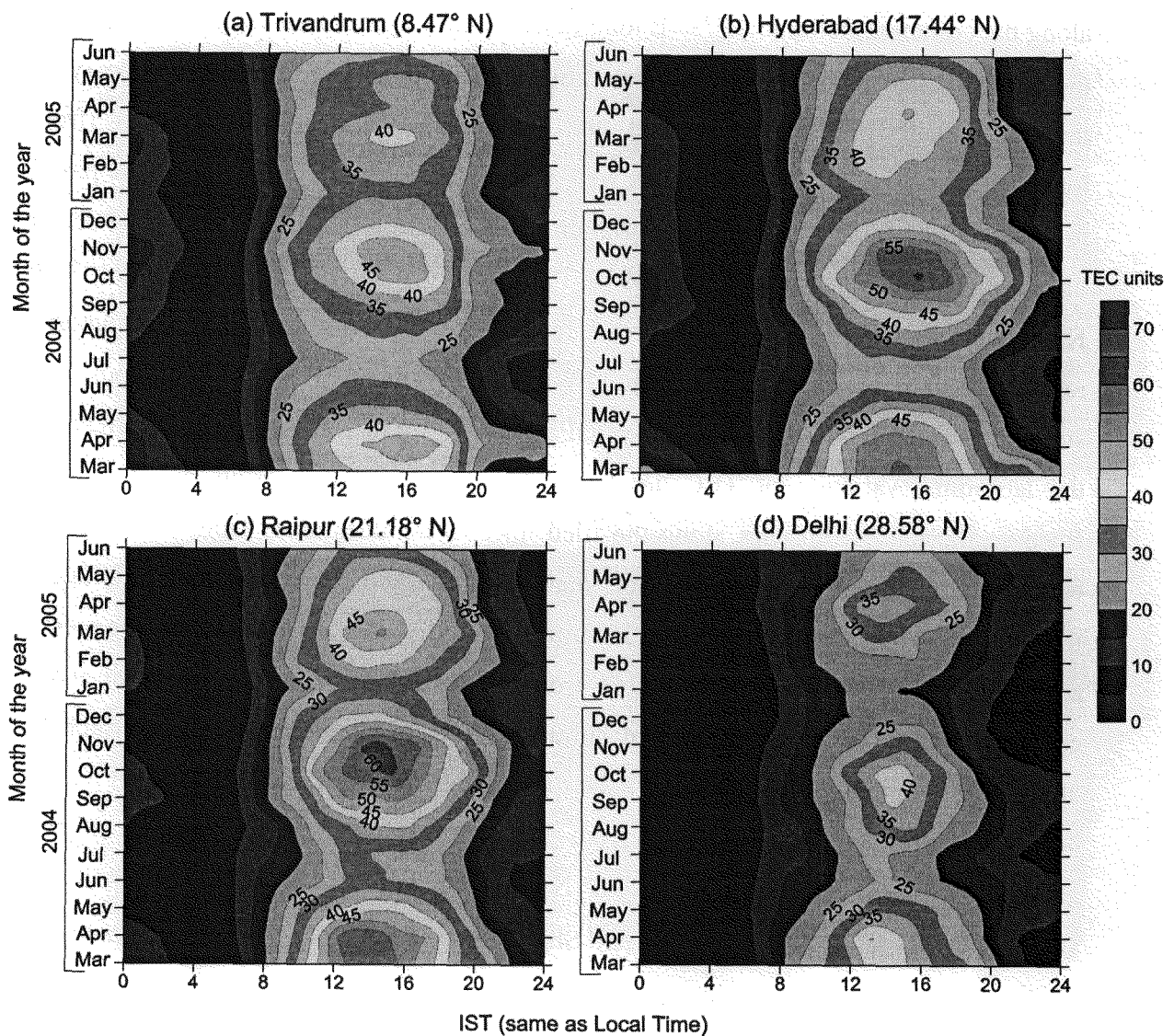

Fig. 22 *Contour plots of the monthly average diurnal variation of TEC at (a) an equatorial station Trivandrum (8.47° N), (b) a sub-tropical station, Hyderabad (17.44° N), (c) an ionization anomaly crest station, Raipur (21.18° N), and (d) a station beyond the anomaly crest, Delhi (28.58° N), during the 16 month period from March 2004 to June 2005 showing significant feature of clear latitudinal and seasonal variation in TEC with equinoxial maxima.*

3.6 Latitudinal variation of the total electron content in the Indian sector:

An interesting feature in the geographic location of India is that the magnetic equator passes through the bottomside tip of the country and the northern crest of the equatorial ionization anomaly lies in the middle of the country providing an unique opportunity for making studies on the latitudinal variation of some of the important ionospheric phenomena such as equatorial ionization anomaly (EIA), Equatorial Ionization and Temperature Anomaly (EITA) and the occurrence of intense scintillations. In the following section, a detailed study on the variation of TEC as a function of latitude in the Indian sector using the simultaneous TEC data from the seven stations chosen along the common meridian of 77° E longitude, all the way from the magnetic equator to the anomaly crest and beyond, is carried out and the results are presented. It may be mentioned here that, from isolated and individual measurements of foF_2 (from ionosonde) and TEC (from orbiting as well as Geostationary satellites) during the past 3 to 4 decades, studies on latitudinal variation of the electron density in the Indian sector have been carried out (Rastogi et al., 1973, 1975; Iyer et al., 1976; Rama Rao et al., 1977; Klobuchar et al., 1977) and the broad features in the behaviour of the equatorial ionization anomaly are brought out. With the availability of a continuous and simultaneous TEC data from the Indian GPS network of stations, a systematic study on the latitudinal variation of TEC has been carried out and the results are presented. Because the plasma diffuses along the filed lines to latitudes away from the magnetic equator in the direction of magnetic meridian, the study will become more appropriate if the data are chosen along the same longitude (to avoid the longitudinal differences if any). Although TEC data is available from all the 18 different locations in India, encompassing different longitude and latitude zones, the data from stations, which lie along a common longitude that covers the maximum latitude extent of the Indian region, are chosen. Hence, the TEC data from the seven stations thus identified, namely Trivandrum (8.47° N), Bangalore (12.95° N), Hyderabad (17.44° N), Raipur (21.18° N), Bhopal (23.28° N), Delhi (28.58° N) and Shimla (31.09° N) along the common meridian of 77° E is considered and the diurnal variation at each of these stations for all the identified quiet days in each of the 16 months from March 2004 to February 2005 are prepared and the results discussed.

Typical diurnal variation plots of TEC for three quiet days namely, 23rd October, 3rd December and 22nd June 2004 from all these seven stations are considered for a preliminary examination and the corresponding contour plots are presented in Figs. 23 (a, b, & c) respectively along with the variation of corresponding EEJ strength. It may be seen from these figures that the day maximum value of the total electron content (TEC) increases from equator to the anomaly crest region (Raipur/Bhopal) and decreases significantly at stations Delhi and Shimla, which lie outside the anomaly crest region. It may also be seen from these figures that the magnitude of the TEC on the equinoxial day (23rd October 2004) is maximum followed by the winter day (3rd December 2004) and is minimum during the summer day of 22nd June 2004. The maximum electron content of 70 TEC units occurs during the local time of 13:00 to 15:00 hrs and maximizes around the geographic latitudes of 21° to 24° N i.e., around Raipur and Bhopal on the equinoxial day of 23rd October 2004. On this day, the equatorial electrojet strength (ΔH) plotted as a function of local time also shows a broad peak with a maximum ΔH value of 62 and an integrated EEJ strength ($\Sigma \Delta H$) of 442 as may be seen from the plot presented under the same figure (27a) indicating that, the higher the electrojet strength, the higher the altitude to which the plasma is lifted at the equator and the farther is the location of the crest of the equatorial ionization anomaly. From Fig. 23(b) i.e., 3rd December, it may be seen that the maximum electron density of 60 TEC units occurs around 16:00 hrs local time at a geographic latitude of about 17° N (i.e., around Hyderabad). The corresponding equatorial electrojet on this day shows a peak value of 55 with an integrated EEJ strength of 326, suggesting that both the magnitude and the latitude of the location of the anomaly crest decreases with the decrease in the electrojet strength. On 22nd June 2004 which represents a typical summer day, (which is also a quiet day with Ap = 2) the contour diagram of TEC drawn as a function of local time and latitude presented in Fig. 23(c) did not show the formation of the crest of equatorial ionization anomaly, but on the other hand showed that the peak TEC value reduces to 30 TEC units and maximizes between 12:00 to 16:00 hrs LT closer to the equator. On this day, typically the electrojet showed a maximum value of 23 with an integrated strength of EEJ of 4, clearly indicating that the EEJ plays a major role i.e., the larger the electrojet strength, the greater the strength of the anomaly crest and the farther is its location and vice-versa.
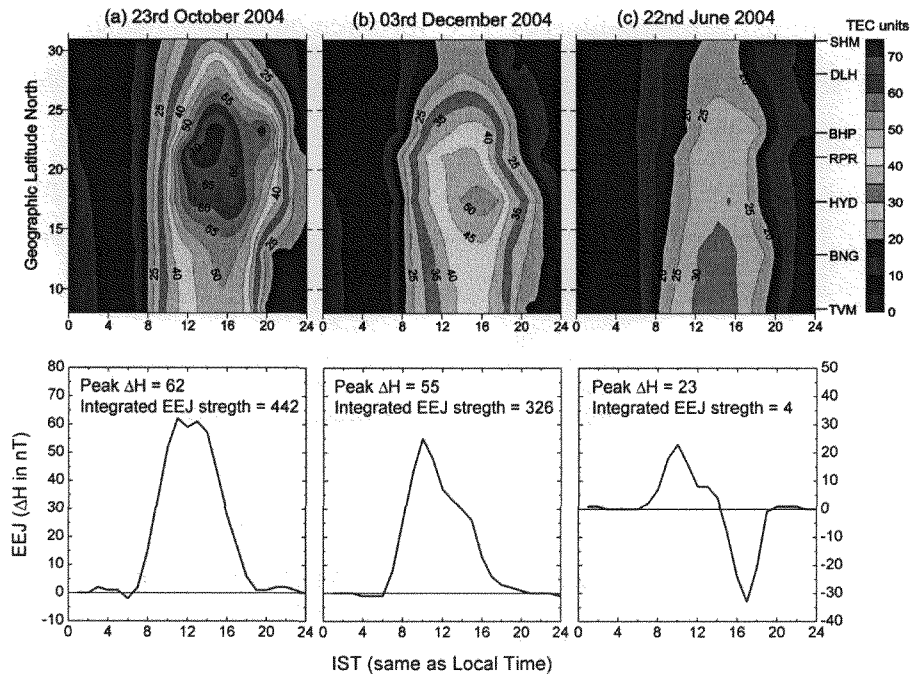
Fig. 23   Typical *Contour plots of the diurnal variations of TEC drawn as a function of geographic latitude (seven stations on a common meridian of 77 E longitude) for (a) an equinoxial day, 23rd October 2004 (b) a winter day, 3rd December 2004 and (c) a summer day, 22nd June 2004 along with the corresponding diurnal variations of the equatorial electrojet strengths.*
The stations are indicated by TVM - Trivandrum (8.47), BNG - Bangalore (12.95), HYD - Hyderabad (17.44), PRP - Raipur (21.18), BHP - Bhopal (23.28), DLH - Delhi (28.58), SHM - Shimla (31.09)
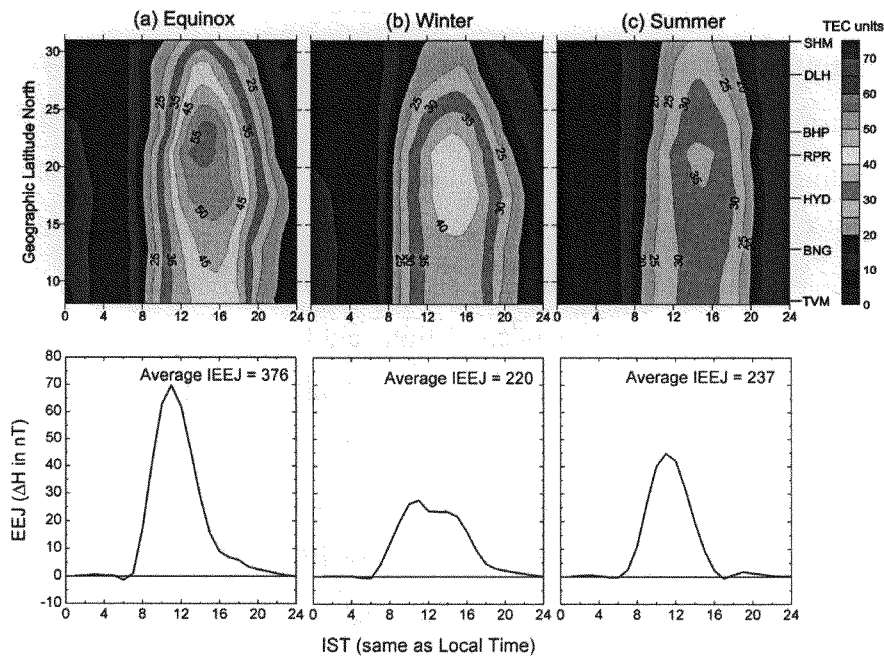

Fig. 24   *Contour plots showing the seasonal average diurnal variations as a function of geographic latitude during the quiet days of the three seasons (a) equinox, (b) winter and (c) summer at the seven stations chosen along the common meridian of 77° E longitude. In the bottom panel is presented the corresponding average diurnal variations of the integrated equatorial electrojet (IEEJ) strength for comparison.*

50

The broad features in the seasonal variation of the equatorial ionization anomaly in TEC are studied preparing the monthly average diurnal variation plots of TEC for each day in each of the 12 months from March 2004 to February 2005 for all the quiet days at the seven identified stations specified earlier, for further examination. From the contour diagrams of TEC drawn as a function of local time versus latitude prepared from the monthly mean values of TEC are presented season wise, along with the corresponding average EEJ strengths. Fig. 24(a) shows these variations in TEC for the set of four equinoxial months i.e., March, April, September and October of 2004, where the TEC maximizes between 12:00 to 16:00 hrs LT. From Fig. 24(a) it is seen that the crest of the equatorial ionization anomaly broadly lies in the geographic latitude belt of 15° to 25° N with the peak occurring around 20° to 23° N during the equinoxial months. In general, the crest of the equatorial ionization anomaly in the Indian sector maximizes around the latitudes of Raipur (21.18° N) and Bhopal (23.28° N) often starting from the latitudes around Waltair (17.7° N) and Hyderabad (17.44° N). The average electrojet strengths presented along with this figure for the corresponding equinox months also show higher values of EEJ justifying the strength and location of the crest of the equatorial ionization anomaly. Similar plot for the months of November, December 2004 and January, February 2005 representing winter months is presented in Fig. 24(b). Here again similar features are also seen but with much reduced intensity in the electrojet strength and TEC as well as in the location of the crest of the anomaly moving equaterward. Whereas, during the summer months of May, June, July and August 2004, the ionospheric plasma densities are in general lower at low latitudes and the formation of the crest of the equatorial ionization anomaly is weak and is almost absent as may be seen from Fig. 24(c). However, the corresponding average electrojet strength is relatively higher compared to those of the winter months. This ambiguity may probably be attributed to the lower ambient electron densities during the summer months owing to the reduced production rates as indicated by the reduced O/N_2 ratios (Titheridge, 1974).

3.7 Relation between equatorial Ionization Anomaly (EIA) and the Equatorial Electrojet (EEJ):

The intensity and location of the equatorial ionization anomaly appears to be mainly dependent on the strength and duration of the equatorial electrojet. In the present study the results strongly suggest a positive relation between EIA and the integrated strength of the EEJ. Therefore it is thought worthwhile to examine whether there is any quantitative relation that can be derived from these observed results. Hence, two

approaches have been tried using the values of the IEEJ (Σ ΔH) and the anomaly strength in TEC and the IEEJ strength and the crest location. That is to find a relation between the anomaly crest location in latitude and the corresponding Integrated Equatorial Electrojet strength IEEJ (Σ ΔH), and the other to find a similar relation between the peak value of the TEC at the anomaly crest region and the corresponding integrated diurnal IEEJ strength.

In Fig. 25(a) is presented the latitudinal location of the crest of the equatorial ionization anomaly as a function of the IEEJ strength. It may be seen from this figure that the location in the crest of the EIA varies from a minimum of 17° N to a maximum of 25° N while the corresponding IEEJ varies from a minimum of 150 nT to a maximum of 650 nT and shows a clear linear relation between them. Similarly, the strength of the EIA (peak TEC value at the crest) as a function of the IEEJ is presented in Fig. 25(b). It is also seen from this figure that there exists a similar linear relation showing that the strength of the EIA increases with the increase of the IEEJ strength. Further, it may be noticed from these two figures (Figs. 25(a) & (b)) that there is a considerable spread in the points on either sides of the regression lines which may be attributed to the effects of other additional processes and phenomena, such as the day to day variation in the neutral winds and local electric fields added to the control of the EEJ on the EIA.
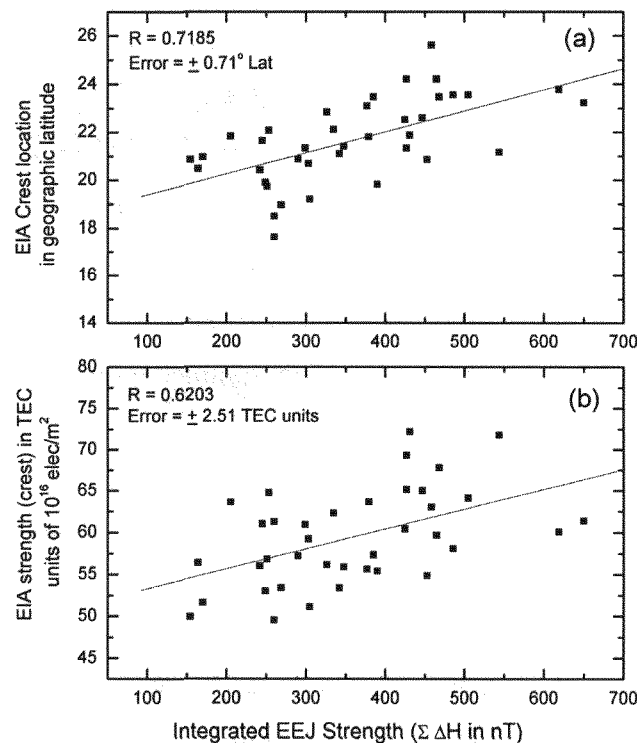

Fig. 25 *Plots showing* (a) *the variation in the geographic latitudinal location of the crest of the equatorial ionization anomaly (EIA) and* (b) *the variation of the strength of the anomaly crest (in TEC units) as a function of the IEEJ strength ($\Sigma \Delta H$ in nT)*

3.8 Latitudinal variation in the formation of the northern crest of equatorial ionization anomaly in the Indian region:

The establishment of the network of the 18 GPS receivers under the GAGAN project in the Indian sector has given an unique opportunity for making continuous and simultaneous measurements of TEC, a comprehensive information of which is of vital importance in the space weather related applications such as Satellite Navigation and Communication Systems. In Fig. 26(a) is presented the vertical TEC (VTEC) values measured during the local time of 09:30 hrs from the GPS network of receivers from all the 18 stations over the entire country on a typical quiet day of 23rd October 2004. It may be seen from this figure that the TEC is in the building-up stage and shows higher values over the equatorial region compared to the latitudes away from the equator. The colour codes of the dots in the figure indicate the strength of TEC at different locations in India. As the day advances, the electric fields increase, increasing the vertical drifts at the equator and give rise to the movement of the plasma to higher altitudes. Around late afternoon hrs i.e., at 15:30 hrs LT, on this day the equatorial ionization anomaly is fully developed, as may be seen from Fig. 26(b). In this figure the higher TEC values (red dots) are accumulated in the geographic latitude zone of 15° to 25° N (i.e., 5° to 15° N geomagnetic latitudes), clearly showing the formation of the EIA in the Indian northern latitudes as has already been presented earlier using the seven stations data chosen along the common meridian of 77° E. Here, this diagram [26(a) and (b)] shown along with the background map of the Indian region, using data of all the 18 stations, gives an overall picture in the development of EIA in this part of the globe and will be of interest for the users in anticipating and evaluating the range delays.
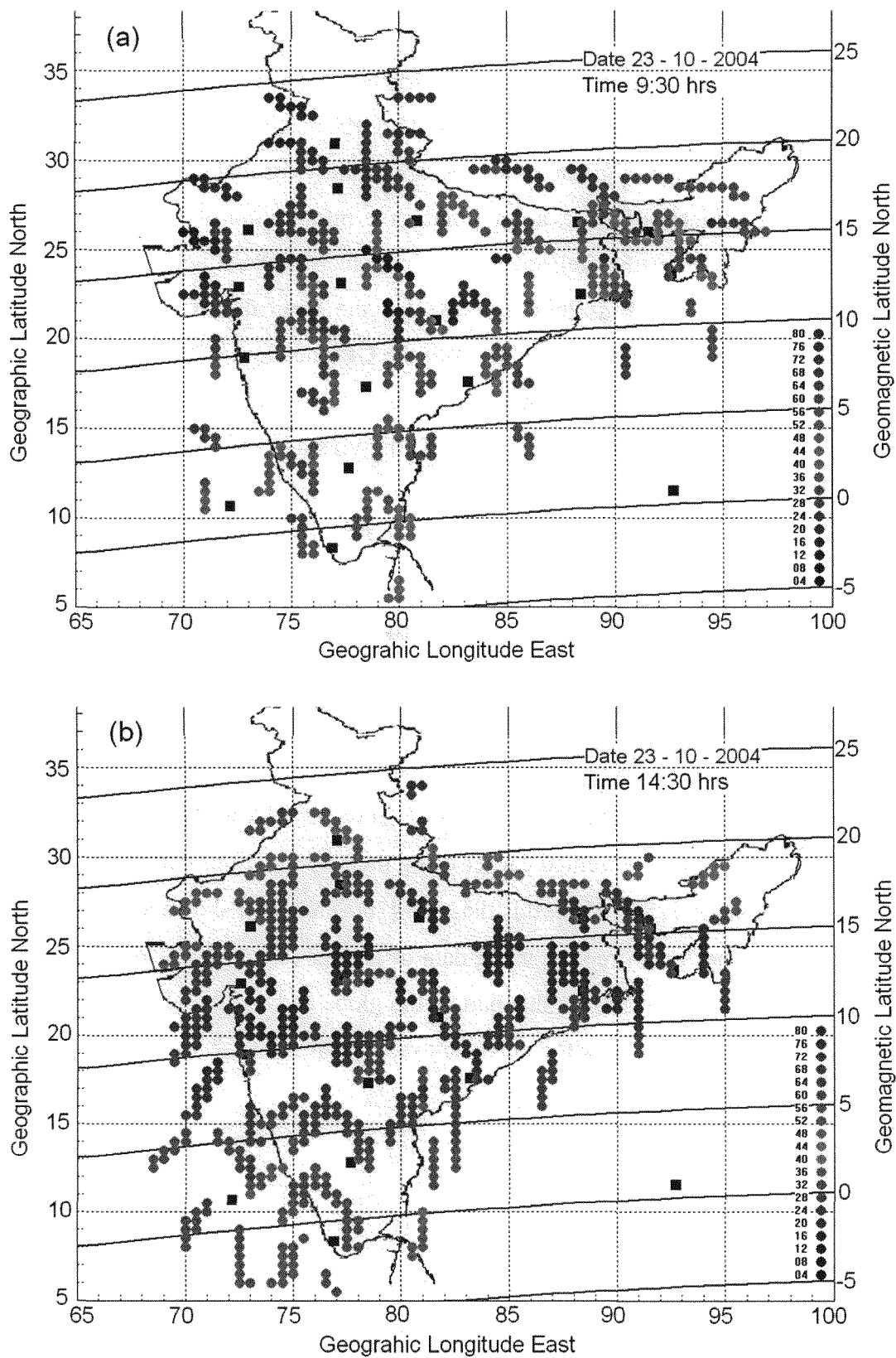
Fig. 26   *Variation of TEC over the Indian latitudes* (a) *during the building up stage of TEC (from 09:00 to 10:00 hrs LT) and*
(b) *during the local time (14:00 to 15:00 hrs) when the EIA is fully developed and confines to 15 to 25 °N geographic latitudes.*
The colour codes represent the strengths of TEC.

3.9 Summary:

The diurnal variation at the EIA region reaches its maximum value between 13:00 and 16:00 hrs LT, whereas near the equator the day maximum is broad and its peak is delayed and occurs around 16:00 hrs LT. Similarly, the day minimum in TEC occurs between 05:00 and 06:00 hrs LT at all stations from equator to the EIA crest region. However, beyond crest region an extended day minimum is found to occur which is flat during most of the nighttime hours i.e., from 22:00 to 06:00 hrs LT, a feature which is similar to that at mid-latitudes. The diurnal variation in TEC shows a minimum to maximum variation of about 5 to 50 TEC units at the equator and from 5 to 90 TEC units at the EIA crest region. These TEC values correspond to range delay variations of about 1 to 8 metres at the equator and about 1 to 15 metres at the crest region, at the GPS-L1 frequency of 1.575 GHz. These variations in the range delays will certainly go up in high sunspot activity (HSSA) periods. The day to day variability in TEC is also significant at all the stations particularly during daytime hours, with maximum variation at the EIA crest regions. Further, it is noticed that the day to day variability in the corresponding EEJ strengths are equally significant in effecting the day to day variations in TEC. Also the location of the EIA crest and its peak value in TEC increases with the increase in the integrated equatorial electrojet (IEEJ) strength.

The monthly average diurnal variations show that the TEC maximizes during the equinox months followed by winter months, and are lowest during summer months. The lower values of TEC during the summer months may be attributed to the low ionization densities due to the reduced production rates (indicated by O/N_2 ratio) owing to the increased scale height of N_2 (Titheridge, 1974).

3.10 References:

Ackroyd, N., and Lorimer, R.: A GPS User's Guide, Lloyd's of London Press, 1990.

Chandra, H. and Rastogi, R.G.: Geomagnetic storm effects on Ionospheric drifts and the equatorial E over the magnetic equator, Indian Journal of Radio and Space Physics, 3, 332-336, 1974.

Coco, D.: GPS - Satellites of Opportunity for Ionospheric Monitoring, GPS World, 47, 1991.

Dasgupta, A., and Basu, A.: Investigation of ionospheric electron content in the equatorial region as obtained by orbiting beacon satellites, Ann. Geophysicae,

29409 – 29419, 1973.

Davies, K., and Hartmann, G.K.: Studying the ionosphere with Global Positioning System, Radio Science, 32, 1695-1703, 1997.

Davies, K., Donnelly, R.F., Grubb, R.N., and Rama Rao, P.V.S.: ATS-6 satellite radio beacon measurements at Ootacamund, India, Radio Science, 14, 85-95, 1979.

Davies, K., Recent progress in satellite radio beacon studies with particular emphasis on the ATS-6 Radio beacon experiment, Space Science Review, 25, 357-430, 1980.

Hocke, K., and Pavelyev, A.G.: General aspect of GPS data use for atmospheric science, Advances in Space Research, 27, 1313-1320, 2001.

Iyer, K.N., Deshpande, M.R., and Rastogi, R.G.: The equatorial anomaly in ionospheric total electron content and the equatorial electrojet current strength, Proc. of Indian Academy of Science, 84, 129-138, 1976.

Kane, R.P.: Irregular variations in the global distribution of total electron content, Radio Science, 15, 837-842, 1980.

Kane, R.P.: Irregular variations in the global distribution of total electron content, Radio Science, 15(4), 837-842, 1980.

Klobuchar, J.A., Iyer, K.N., Vats, H.O., and Rastogi, R.G.: A numerical model of equatorial and low latitude total electron content for use by satellite tracking systems for ionospheric corrections, Indian Journal of Radio and Space Physics, 6, 159-164, 1977.

Klobuchar, J.A.: "Ionospheric Effects on GPS", in "Global Positioning System: Theory and Applications, Vol 2", edited by Parkinson, B.W., and Spilker, J.J., Progress in Astronautics and Aeronautics, Vol.164, page 485, 1996.

Langley, R., Fedrizzi, M., Paula, E., Santos, M., and Komjathy, A.: Mapping the low latitude Ionosphere with GPS, GPS World, 13 (2), 41-46, 2002.

Mannucci, A.J., Wilson, B.D., and Edwards, C.D.: A new method for monitoring the earth's ionospheric total electron content using the GPS global network, Proc. of ION GPS-93, Inst of Navigation, 1323-1332, Sept 1993.

Mendillo, M., Lynch, F.X., and Klobuchar, J.A: Solar Terrestrial Predictions, vol. 4, edited by Donneylly, R.F., Space Environment Lab, Boulder, Colorado, USA, C1- C14, 1980.

Modi, R.P., and Iyer, K.N.: IEC and slab thickness near the peak of equatorial anomaly during sunspot maximum and minimum, Indian Journal of Radio and Space

Physics, 18, 23-26, 1989.

Rama Rao, P.V.S., Gopi Krishna, S., Niranjan, K., and Prasad, D.S.V.V.D.: Study of Spatial and temporal characteristics of L-band scintillations over the Indian low latitude region and their possible effects on GPS navigation, Annales Geophysicae, 24, 1567-1580, 2006.

Rama Rao, P.V.S., Srirama Rao, M., and Satyam, M.: Diurnal and seasonal trends in TEC values observed at Waltair, Indian Journal of Radio & Space Physics, 6, 233-235, 1977.

Rastogi, R. G., and Sharma, R. P.: Ionospheric electron content at Ahmedabad (near the crest of equatorial anomaly) by using beacon satellite transmissions during half a solar cycle, Planetary and Space Science, 19, 1505 – 1517, 1971.

Rastogi, R.G., Iyer, K.N., and Bhattacharyya, J.C.: Total electron content of the ionosphere over the magnetic equator, Current Science, 44, 531-533, 1975.

Rastogi, R.G., Sharma, R.P., and Shodan, V.: Total electron content of the equatorial ionosphere, Planet Space Science, 21, 713-720, 1973.

Soicher, H., and Gorman, F.J.: At middle & high latitudes, soicher and Gorman observed day to day variability is less than 25% irrespective of location, Proceedings of COSPAR Satellite Beacon Symposium, Warsaw, Poland, 91, 1980.

Sonnenberg, S.: Radio and Electronic Navigation, Chapter 7, Butterworth and Co, 6th Edition, 1988.

Titheridge, J.E.: Changes in atmospheric composition inferred from ionospheric production rates, Journal of Atmospheric and Terrestrial Physics, 36, 1249-1257, 1974.

Van Dierendonck, A.J., Fenton, P., and Klobuchar, J.: Commercial ionospheric scintillation monitoring receiver development and test results, Proceedings of the Institute of Navigation's 52nd Annual Technical Meeting, Cambridge, MA, 573 - 582, 1996.

Wanninger, L, "Effects of the Equatorial Ionosphere on GPS", GPS World, page 48, July 1993.